



# A Simple Time-Dependent Chart of Extension Fracture Initiation within Brittle Homogenous and Heterogeneous Rock Pillars in Hard Rock Mining

Fhatuwani Sengani 

Received: 19 August 2019 / Accepted: 5 January 2020 / Published online: 16 January 2020  
© Springer Nature Switzerland AG 2020

**Abstract** A simple empirical time-dependent chart of extension fracture initiation is described. The chart was developed using simple borehole periscope observations within the rib pillars, focusing on monitoring the initiations of extension fracture. Nevertheless, the periscope was conducted time to time for the duration of a month, within brittle homogenous and heterogeneous rock pillars (rib pillar). The chart is suitable for predicting extension fracture initiations and extends of fracturing as time progress, predicting the allowable time to install an effective support system and be able to estimate the stability of the rib pillars within a brittle homogenous and heterogeneous rib pillars in a high stress environment. Two practical application and examples of the chart are described. These are firstly, an alternative way of estimating the rib pillar strength and secondly, predicting the maximum allowable time for an effective support installation along the rib pillar.

**Keywords** Extension fracture · Brittle rock mass · Homogenous rock pillar · Heterogeneous rock pillar · Hard rock mining

## 1 Introduction

Rock related fatalities and injuries are still reported at an alarming rate in South Africa's deep to ultra-deep level hard rock mining (Department of Mineral Resources (DMR) 2018). Most of these events are associated with Falls of the Ground (gravitational and rock burst). As a result researchers have been called upon to provide solutions to the problem, given that, most solutions were in the form of numerical approximation of the rock behaviour, requesting critical skills given to young rock engineers and seismologists (Tooper 2003; DMR 2018). Besides that, the complex behaviour of the rock and rock mass has been extensively reported (Stacey and Yathavan 2003; Stacey et al. 2007), specifically rock fracturing (Huang et al. 2017; Xu et al. 2018; Zhang et al. 2017; Zhou et al. 2018) which is believed to be an under studied behaviour of the rock mass (Stacey 1981; Hamm et al. 2007; Reeves et al. 2013; Ren et al. 2015, 2017; Wesseloo and Stacey 2016; Ren and Santamarina 2018). The understanding of rock fracturing and rock damage is very crucial in order to predict the rock pillar behaviour with time (Earon and Olofsson 2018;

---

In this paper, the term chart is sometimes referred to three charts that are similar but differ with the composition of the rock pillar, sometimes it is referred as charts which means chart for homogenous heterogeneous (single structure) and heterogeneous (multiple structure) rock pillar.

---

F. Sengani (✉)  
Department of Geology and Mining, University of Limpopo, Private Bag X1106, Sovenga, Polokwane 0727, South Africa  
e-mail: Fhatuwani.sengani@ul.ac.za;  
fhatugeorge@gmail.com

Sengani and Zvarivadza (2018a). In support of this, Cai and Kaiser (2018) have also confirmed that rock fracturing is a significant tool used for support design by predicting the depth of fracturing relative to support design. Nevertheless, rock fracturing is simple mechanical breaks that occur in a rock unit, in which discontinuities in displacement across surfaces or narrow zones are involved. Historically, rock fractures have been grouped into three categories; dilating fractures/joints (Lawn and Wilshaw 1975; Pollard and Aydin 1988; Lee et al. 1995; Pan et al. 2010), shearing fractures/faults (Barton 1983; Dyer 1983; Segall and Pollard 1983a, b; Zhao and Johnson 1992) and closing fractures/pressure solution surfaces (Bates and Jackson 1980; Nelson 1985). Rock fracturing, as well as rock fracture propagation and distribution, have been associated with the concepts of stress concentration, amplification, and energy balance, which are dated back to Inglis (1913) and Griffith (1921). Traditionally, Griffith, Mohr criteria and Stacey's Extension strain criterion are the three common hypotheses used to evaluate rock fracturing initiation within a brittle rock mass at the vicinity of underground excavations (Clausing 1959; Stacey 1981; Wesseloo and Stacey 2016). One fundamental issue that remains fully unsolved is the accurate prediction of rock fracturing at high-stress levels using these conventional criterions/hypotheses mentioned above. The traditional hypotheses are briefly described in the subsection below.

## 2 Theoretical Background on Rock Fracture Initiations

### 2.1 Griffith and Mohr Criteria

Griffith (1921) conducted an experiment using glass samples to understand the fracturing of solid material by applying stress level much lower than the theoretical strengths of glass. Griffith then attributed this to the amplification of stress around flaws in the glass, which is well known as stress concentration. As a result, Griffith (1921, 1924) proposed a non-linear criterion based on the initiation of fracture in brittle materials. Nevertheless, the original work by Griffith (1921) focused on fracture initiations in a material subjected to tensile stress. However, Griffith extended the first concept and included biaxial compression

loading (Griffith 1924). The equation governing the tensile failure in a biaxial compressive stress field is given in Eq. 1 (Griffith 1924);

$$\sigma_1 = \frac{-8\sigma_t \left(1 + \frac{\sigma_3}{\sigma_1}\right)}{\left(1 - \frac{\sigma_3}{\sigma_1}\right)^2} \quad (1)$$

where  $\sigma_t$  is the uniaxial tensile strength of the material,  $\sigma_1$ ,  $\sigma_3$  are principal stresses. Note that tensile stresses are negative.

Orowan (1949) provided a simple interpretation of Griffith's theory in this manner; "*fracture initiates when tensile stress-induced at or near the tip of an inherent crack exceeds the molecular cohesive strength of the materials*". Since the molecular cohesive strength is difficult to determine using direct measurements (Hoek 1965), therefore, Hoek (1964) indicated that the fracture criterion was then expressed in terms of the uniaxial tensile strength of the material. Besides the successfulness of the criterion, a serious limitation of Griffith's theory lay in the fact that it can only be used to predict fracture initiation and yields no information on the rate or direction of the fracture propagation (Hoek 1965). Furthermore, the theory was based on the energy consideration and Griffith's equations consisting of surface energy. Due to the difficulties experienced when evaluating the surface energy of the material, this criterion (Griffith's theory) was later modified by several authors (Brace 1960, 1964; McClintock and Walsh 1962; Murrell 1963, 1965; Erdogan and Sih 1963; Hoek 1964; Jaeger et al. 2007; Wei et al. 2018; Andriev 1995; Paterson and Wong 2005), the modified approaches considered the stress concentration at the crack tip.

Extensive contribution to the theory was made by Murrell (1958) in which the author proposed the application of Griffith theory to a rock. Murrell (1958) extended Griffith's two-dimensional theory to three-dimensions. The modification involved detailed evaluation of the stress-induced at the vicinity of the open penny-shaped cracks within a semi-infinite body subjected to triaxial compressive stresses  $\sigma_1$ ,  $\sigma_2$ , and  $\sigma_3$ . The study reported that no significant influence of the intermediate principal stress on the crack tip stresses induce tensile failure initiation. As a result, the modification criterion was noted to be like a concept of loading a penny-shaped crack in a biaxial stress field. The equation governing the modification by the above

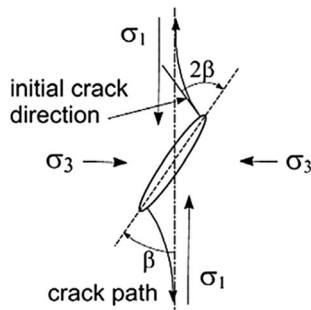


**Fig. 1** Tensile crack propagation from an inclined elliptical Griffith crack in a biaxial compressive stress field (after Hoek and Martin 2014) where  $\sigma_t$  is the uniaxial tensile strength of the material and  $\sigma_1, \sigma_3$  are principal stresses

author is shown in Eq. 2 and the description is shown in Fig. 1;

$$\sigma_1 = \frac{-12\sigma_t \left(1 + 2\frac{\sigma_3}{\sigma_1}\right)}{\left(1 - \frac{\sigma_3}{\sigma_1}\right)^2} \tag{2}$$

As a matter of fact, the theory has gained more interest among several authors such as Cho et al. (2007), while some of the authors considered to further the understanding of theoretical studies on closed cracks according to the theory including authors such as Fairhurst (1964, 1972), Ashby and Hallam (1986), Kemeny and Cook (1987), Germanovich and Dyskin (1988), Martin et al. (1997) and Cai et al. (1998). Fairhurst (1972) is one of the recommended studies which briefly outlines the application and principle behind the theory.

A recent study by Wei et al. (2018) titled “An Improved Crack Initiation Stress Criterion for Brittle Rocks under Confining Stress” has shown a significant contribution in the field of fracture mechanics. The authors conducted uniaxial and triaxial compression tests on two sets of hard sandstones, and their experiments involved the dilation strains and AE counts to characterise the crack accumulation. Owing to this, crack initiation stress was determined using the inflection point on the strain and AE curves. As a result, the study concluded that the new criterion can predict the crack initiation stress of confined rock with high accuracy.

On the other hand, the theory has received some criticism where arguments by Handin et al. (1967) reported that both Griffith, as well as the modified theories such as the Mohr criteria, focus on the concept

of stress rather than the fracture initiation. Handin et al.’s (1967) argument was based on a series of compression, torsion and tension tests where the results have shown that there is no appropriate criterion in terms of “*stress alone for macroscopic fracture in the brittle region*”. The study (Handin et al. 1967) concluded that both the Mohr and Griffith criteria were found to be inadequate at low-stress conditions. Yet, it has been observed on several occasions that the failure of intact rock occurs when the in situ principal stress is far less than the rock uniaxial compressive strength (Stacey 1981; Wesseloo and Stacey 2016).

### 2.2 Stacey’s Extension Strain Criterion

Decades later, an alternative way of identifying the extent and orientation of extension fractures ahead of the mining faces was then presented by Stacey (1981), in which a criterion well known as “Stacey’s Extension strain criterion” was reported to successfully predict both orientation and extent of fractures. Stacey’s criterion outlined that “... *fracture of brittle rock will initiate when the total extension strain in the rock exceeds a critical value which is characteristic of that rock type*”. The equation governing the criterion is shown in Eq. 3.

$$e \geq e_c \tag{3}$$

Stacey (1981) furthered his discussion by providing an equation which is applicable for materials that are ideal for linear deformation behaviour, where the equation is based on minor strain, in which the strain is presented in the direction related to the three principal stresses.

$$\varepsilon_3 = \frac{1}{E} [\sigma_3 - \nu(\sigma_1 - \sigma_2)] \tag{4}$$

Stacey (1981) concluded that the criterion is applicable in a brittle rock mass, but it is not expected that the criterion is applicable in all conditions of stress or all types of rock. The previous author also outlines some of the cardinal points which show that since fracture depends on the extension strain; therefore, the criterion is expected to be applicable at the vicinity of the excavations in a rock.

The criterion has also gained extensive interest which includes recent researchers (Waldeck 1979; Stacey 1982, 1989; Stacey and Harte 1989; Pang and

Goldsmith 1990; Stacey et al. 2003; Ndlovu 2006; Ndlovu and Stacey 2007; Steffanizzi et al. 2007; Andersson et al. 2009; Nicksiar and Martin 2012; Li and Wong 2013). In summary, the above studies have reported that the extension strain criterion has a great potential to predict rock fracturing, through the use of laboratory studies, in situ studies and numerical simulations. Although there is reasonable evidence concerning the successfulness of the criterion and its applications, its practical usage has been reported to be limited due to the fact that failure constraint by an extension mechanism is generally not physically possible (Ryder and Jager 2002; Kwásniewski and Takahashi 2010). This led them (Ryder and Jager 2002) to conclude that, “...the extension strain hypothesis has little connection with reality, and in fact (at least in its present form) should not be used”. On the other hand, Kwásniewski and Takahashi (2010) concluded that “Stacey’s criterion was not supported by the test results”. They further outline that although the extension strain criterion does not predict the failure condition well, it may be able to find the application in conditions of low confinement. Ryder and Jager’s (2002) argument has been found to be unrelated to Stacey’s hypothesis because it is based on rock failure rather than fracture initiations.

To this end, there is no specific empirical extension fracture initiation criterion designed for different compositions of brittle rock pillars in high stress ground conditions. Therefore, this limitation motivated this study, on developing new simple time dependent chart on rock fracturing in a brittle rock mass at a high stress environment. The chart was developed based on a thorough revisit of the Stacey’s extension strain criterion for rock fracturing with the focus on relating its application in high stressed brittle rock pillars and to modify the criterion or develop a new criterion. In this paper, the terminology “rib pillar” is sometimes referred to as rock pillar. Like Stacey (1981), the term tensile strain has been exchanged with extension strain since tensile strain might imply the presence of tensile stress. Lastly, the focus of this paper is on the extension fracture initiations rather than rock failure.

### 3 Research Approach

The research has integrated two techniques in order to study the stated problem where the techniques

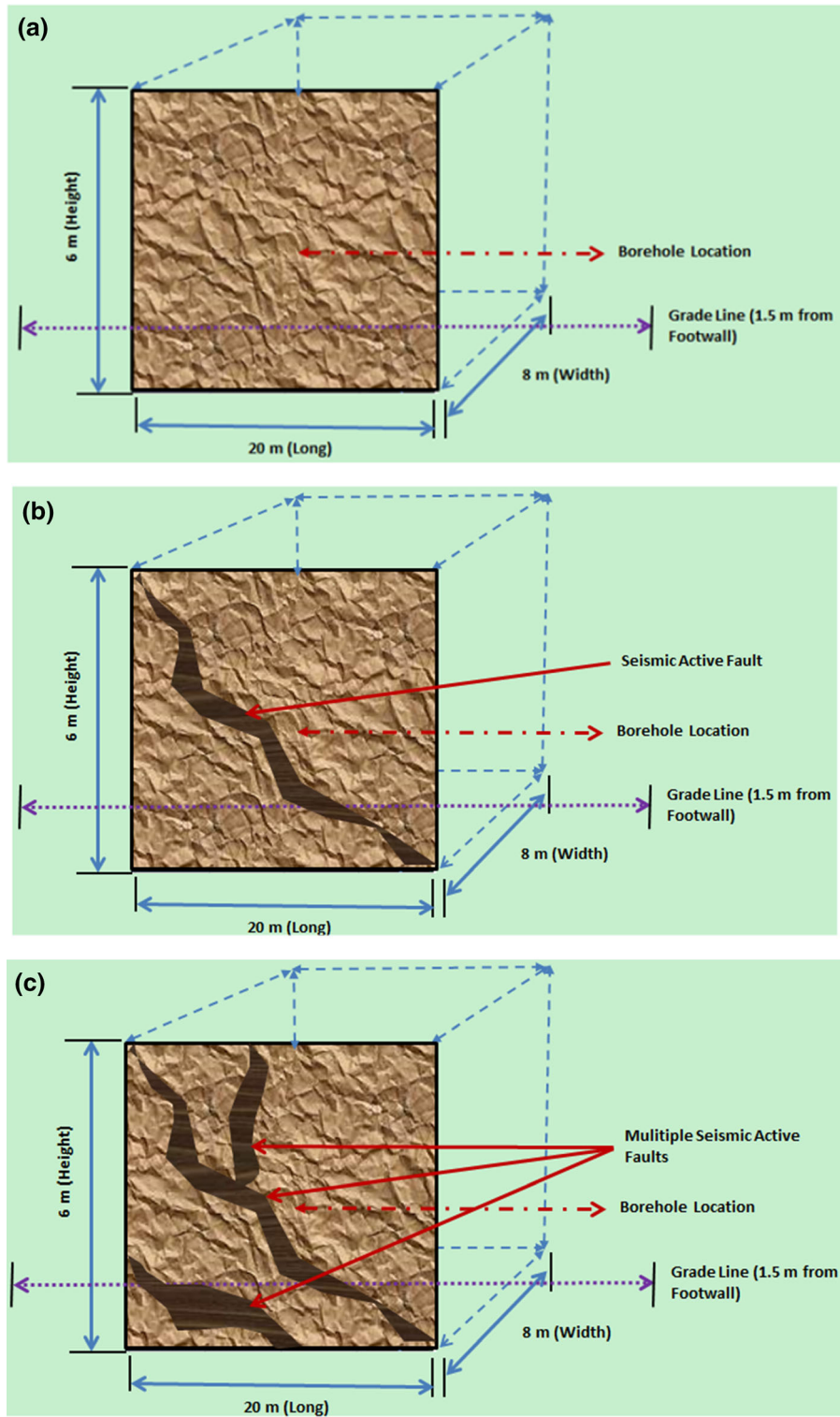
incorporate the following; borehole periscope observations and Ground Penetrating Radar analysis. These techniques have led to the development of extension fracture initiations criteria as well as the development of a time-dependent chart of extension fracture initiations. A brief discussion of each method is outlined in the subsections below.

#### 3.1 Borehole Periscope Observations

Horizontal short boreholes with a maximum depth of 4 m were drilled perpendicular to the length of the brittle rib pillars. The boreholes’ diameter was 55 mm. The brittle rock pillars “rib pillars” composed of large pebble conglomerate (Modderfontein Group) and the dimensions of the rib pillar which were 20 m long (length) and 8 m in width and 6 m in height (Fig. 2a–c). For further reading on geological setting of the study area, the reader is referred to the following studies De Kock (1964), Pretorius (1964, 1986), King et al. (1989), McCarthy (2006) and for further reading on the mining method related to the study, to studies by Watson et al. (2014), Sengani and Amponsah-Dacosta (2018), Sengani (2018a, b), Sengani and Zvarivadza (2018a, b, c). A borehole camera was inserted in a drilled borehole at a very low speed to produce detailed and clear videos and images that could be easily interpreted. The videos and images from the borehole camera were used to study the initiations and extent of extension fractures as time progressed through a comprehensive comparison on the development of extension fractures weekly for a period of 4 weeks. In order to simplify the complexity when studying the development and the extent of extension fractures, a fracture frequency standard table proposed by Sengani and Zvarivadza (2017) was utilised (Table 1).





#### 3.2 Ground Penetrating Radar

A Ground Penetrating Radar was also used to analyse the density of fracturing. From the GPR images, it was possible to study the fracture depth and intensity of fracturing within the brittle rib pillar and two scans were taken from each rib pillar at the completion date of the investigation. One scan was taken below the grade line where there was no support system installed and the second scan was taken above the grade line in which the rib pillar was fully supported. Therefore, in




**Fig. 2** Schematic view of the studied homogenous brittle rock pillar “Rib pillar” with no **a** visible seismic active fault, **b** one visible seismic active fault, **c** multiple visible seismic active faults. Note that the sketch is not in scale

**Table 1** The standard for fracture frequency analysis (Sengani and Zvarivadza 2017)

Fracture frequency/ metre	Risk profile	Colour coding
<5	High strainburst risk, rockmass not fractured/yielded	
5– 10	Medium strainburst risk, rockmass beginning to fracture/yield	
10 – 20	Low strainburst risk, rockmass has fractured/yielded	
>20	Very low strainburst risk, rockmass highly fractured/yielded	

**Table 2** Fracture frequency standard for Ground Penetrating Radar

Fracture frequency/ metre	Risk profile	Colour coding
<5	High strainburst risk, rockmass not fractured/yielded	
5– 10	Medium strainburst risk, rockmass beginning to fracture/yield	
10 – 20	Low strainburst risk, rockmass has fractured/yielded	
>20	Very low strainburst risk, rockmass highly fractured/yielded	

Note that, amplitude and frequency values increases from dark red colour (> 20 fracture frequency/metre) toward dark blue colour (< 5 fracture frequency/metre), while the wavelength reduces from dark red colour toward dark blue colour. In simple terms, a zone with dark red colour represents low amplitude and frequency with very high wavelength, while a zone with dark blue represents high amplitude and frequency with very low wavelength

order to eliminate the error caused by a metallic object (welded mesh and bolts), the frequency of the electromagnetic light was increased in order to ensure that the results are relevant and reliable. The results were simplified by developing a fracture intensity standard using colour coding represented in the scanner. The color-coding table was developed after several scans had been calibrated using results from borehole periscope for known rib pillar behaviour. The colour coding used is presented in Table 2.

### 3.3 Extension Fracture Initiations Criterions

Based on the observations made within different rib pillar composition, a further study on the development

of extension fracture initiations criterion was initiated. It was developed by modifying the previous criterion (Stacey 1981) which ensured that the suggested equations corresponded with the observational point of view on how extension fractures were developed time to time in each rib pillar. Therefore, three equations were then suggested based on the ratio of the developed fractures within the different components of the rib pillar at certain zones. The baseline used was the homogenous rib pillar since it represents a rib pillar with no disturbance, the rest of the rib pillars (heterogeneous rib pillar) were then compared with it. Finally, the ratios were incorporated within the extension fracture equations and the correspondences were fully studied along with all categories of the rib pillars.

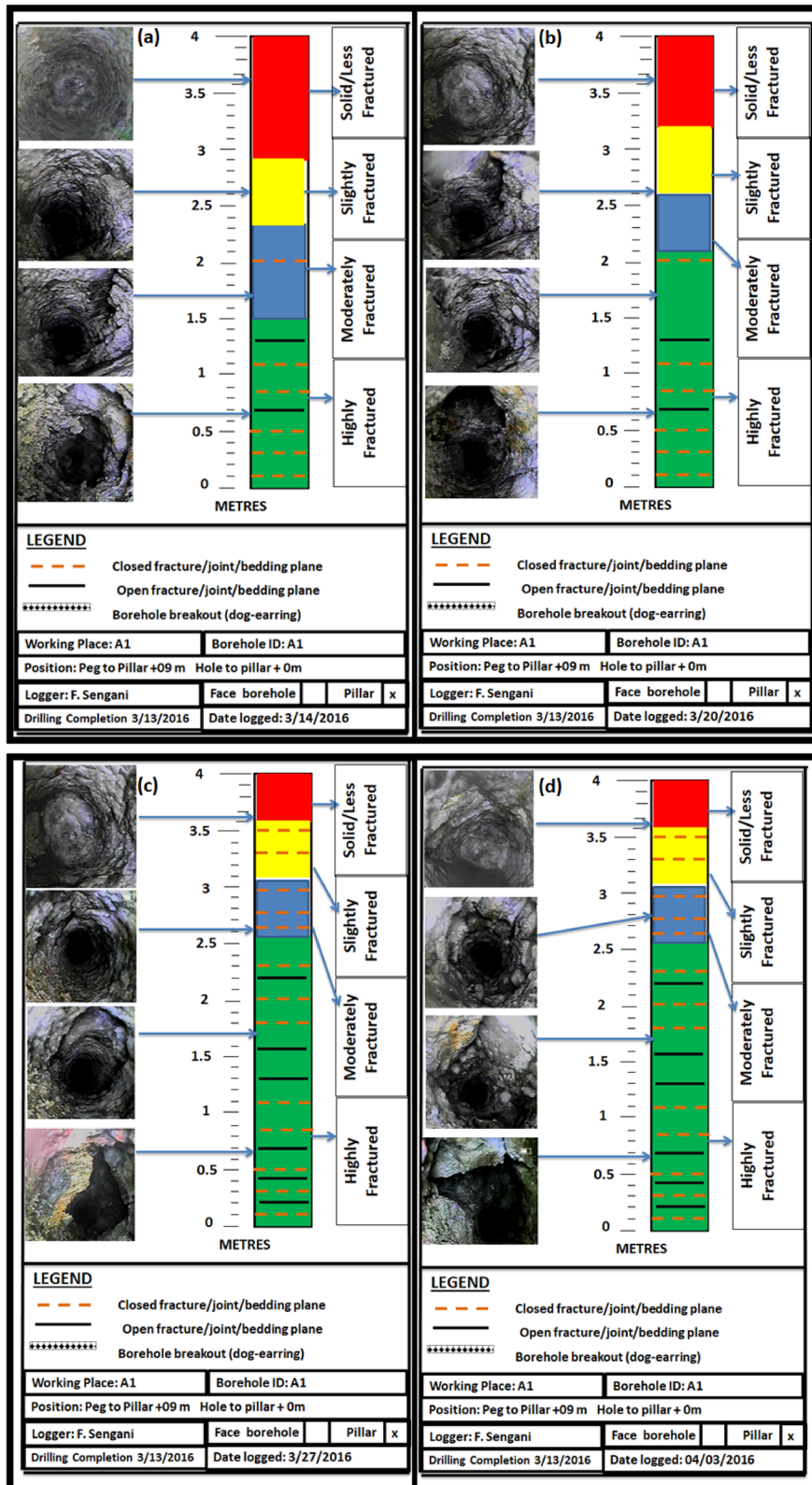


Fig. 3 Borehole periscope observations on the development of extension fracture in a day, b week, c 2 weeks, d 3 weeks, e 4 weeks

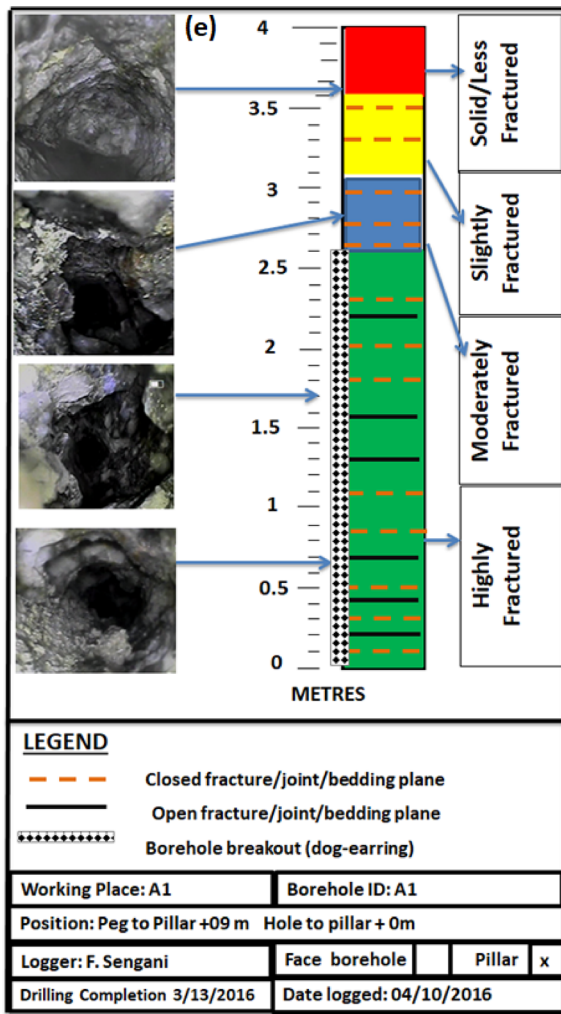


Fig. 3 continued

### 3.4 Time-Dependent Chart of Extension Fracture Initiations

The intention of the study was to develop a time-dependent chart on extension fracture initiations within a brittle homogenous and heterogeneous rock pillar. The chart is based on the observational point of view and empirical analysis and suggested equations on extension fracture initiations from the different compositions of the rib pillars. The average behaviour of several compositions of rib pillars were then described by the chart based on several fractures noted to have developed as time progressed. The chart was adjusted with possible outcomes observed from the several rib pillars and zones defined in the chart in which the expected development

of extension fractures from different rib pillars could be established. Two examples of the application of the chart and equation are presented below.

## 4 Results and Discussion

The results presented in this paper are divided into five sections, the first section presents and discusses the results on the borehole periscope observations on the development of extension fractures within the different components of the brittle rib pillars. The second section presents and discusses the application of the Ground Penetrating Radar when validating the extent of extension fractures along with several compositions of the rib pillars. The third section presents and discusses the suggested equations on the initiation of the extension fractures within the different composition of the brittle rib pillars. The fourth section provides a detail description on the suggested time-dependent chart of extension fracture initiation with time. Lastly, the application of the chart is presented in two different case studies.

### 4.1 Borehole Periscope Observations on the Initiations of Extension Fractures

#### 4.1.1 Extension Fractures Initiation in Homogenous Brittle Rib Pillars

Based on the periscope analysis and results, it was noted that after 24 h (1 day) extensive fracturing (more than 20 fractures) was generally observed from the boreholes collar to the depth of 1.2 m toward the rock pillar core (Fig. 3a). A zone of moderately fracturing (10–20 fractures) was observed from 1.2 m to a maximum depth of 2.1 m, this zone was then followed by slightly fracturing (5–10 fractures) that was observed to occur at the depth of 2.1 m from the borehole collar and to a maximum depth of 2.9 m toward the pillar core and lastly, a solid zone or a zone with fractures less than 5 (see Table 1 for fracture rating) were observed from 2.9 to the pillar core (4 m). These give an indication that the intensity of extension fracturing was decreasing with the depth of the borehole. Nevertheless, the observations from day 1 correspond very well with observations made by other researchers. Louchnikov (2011) applied the extension strain criterion to predict fracturing around the mining



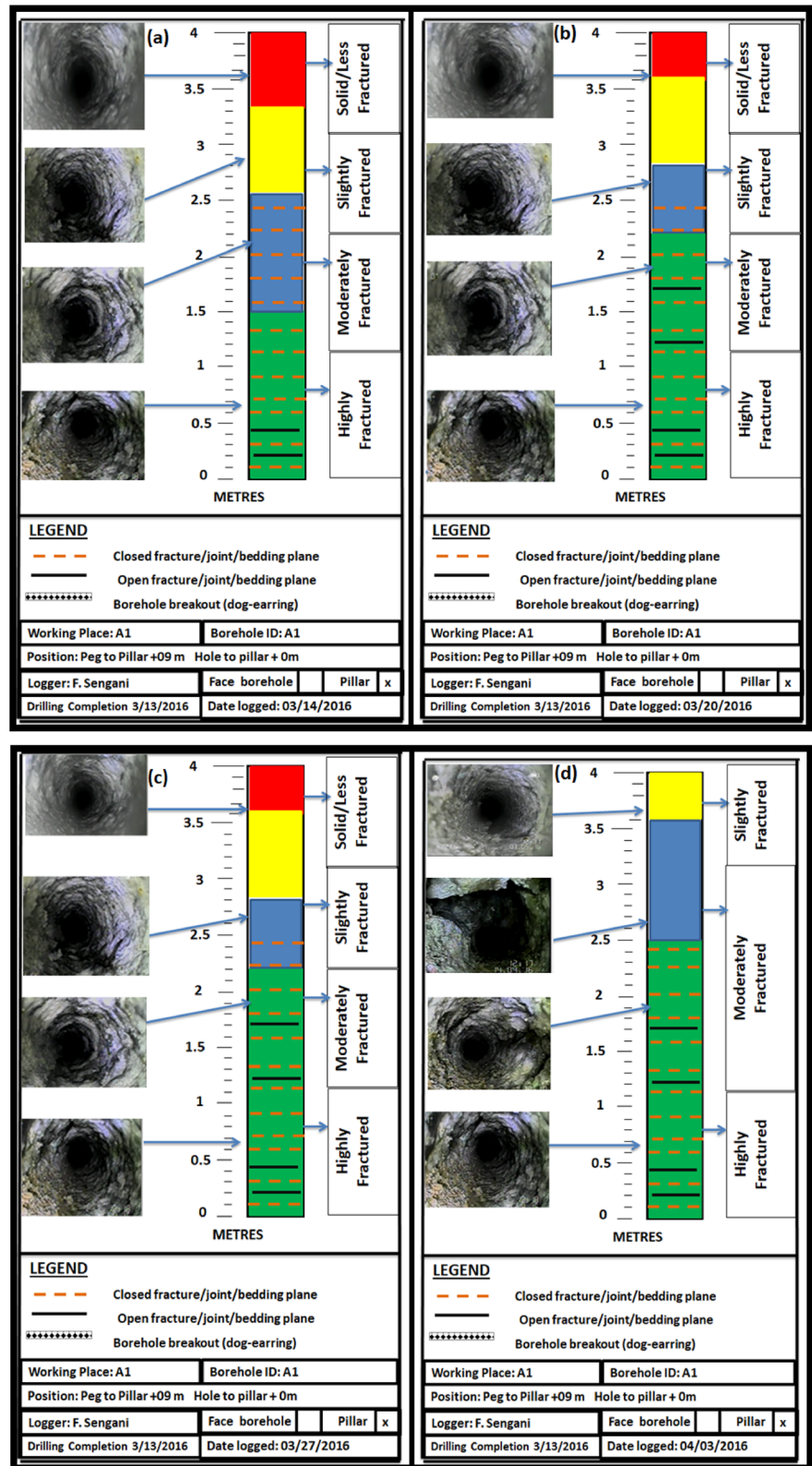
excavations with the purpose of designing a reliable support system. The study has shown the development of fracturing to decrease with depth, the study used the intensity of fracturing on quantifying the potential failure around the mining excavations. Lim and Martin (2010) conducted a study on core diskings relative to fracturing where the study indicated that core fracturing decreases with the depth of the borehole. Furthermore, a conclusion by Lim and Martin outlines that the core fracturing becomes partial diskings or non-diskings towards the end of the borehole, and these results have a linear correlation with the periscope observation from the first day. Van Aswegen and Stander (2012) conducted a study on the “origins of some fractures around tabular stopes in deep South African mines” and their study has shown an impression that different types of extension fractures take place with time, in which relative low number of extension fractures are expected to be represented at an initial stage after blasting. Zvarivadza and Sengani (2018a) and Sengani (2018b) have studied the performance of the in-stope pillar which indicated that the development of fracturing reduces with depth. Nevertheless, studies such as those by Adam and Jager (1980) reported different observations in which the authors indicated that fractures are formed in discrete zones separated by solid rock, meaning that fracturing can be grouped and separated by the solid rock zone in the entire drilled borehole.

After a week, borehole periscope was conducted within the same drilled boreholes from different rib pillars, where extensive fracturing (more than 20 fractures) was observed to be concentrated from borehole collar up to a maximum depth of 2 m. This zone was noted to have both closed (< 1 mm opened) and open fractures (more than 1 mm opened) (Fig. 3b), with most of the previously closed fractures opening up. The intensity of open fractures was observed to reduce as the depth of the borehole increases from 2 to 2.5 m, this zone was moderately fractured with fracture frequency ranging from 10 to 20. Moderate fracturing was observed to occur from 2.5 to 3.1 m, with this zone followed by a solid zone or zone with fractures less than 5, which were observed from 3.1 to 4 m. The observation gives an impression that the extension fracture continues to develop from time to time, and the observation corresponds very well with the several studies such as those conducted by Clotte et al. (1972–1973). The authors contested

that a fracture is developed as a regular progression. Sengani and Zvarivadza (2018a) conducted a study on borehole periscope observation on the development of fracture ahead of the preconditioned mining faces. Their study has also indicated that fractures develop from time to time and extensive fracturing is expected as the time goes by. In actual sense, the study gives an impression that the rock mass properties control the initiations of fracture as time progresses. These results seem to have a slightly different view as compared to the Krauland (1970) model and Stacey (1981) observations, in which the authors estimated a maximum depth of 1.2 m to be the depth in which extension fractures can extend. The disagreement with these two studies concerning the depth as also evidenced in a study by van Aswegen and Stander (2012) in which the author revealed that several types of extension fractures are expected to develop with time due to the stress regime it is subjected to.

The extent and development of new extension fractures were further evidence from 2 to 4 weeks. The occurrence of these extension fractures was in the manner that previously closed fractures which became opened fractures, while the solid zones became disintegrated as time progressed (Fig. 3c–e). The observation made relates very well with the observation made by Kuijpers (2000), who maintained that fracturing in a compressive stress environment is a secondary effect. The study also noted some of the cardinal points that show that primary failure in a rock is a form of micro fracturing and it is assumed to precede to major fractures, which gives an impression that the development of extension fracture is expected to initiate from micro extension fractures, closed and lastly open extension fractures. In evidencing the previous studies, new extension fractures were noted to be developed throughout the borehole as time progressed, with extensive fracturing dominated within the first few meters towards the rib pillar core. In summary, extensive fracturing was observed to gradually increase as the duration of the investigation progressed meanwhile closed fractures were noted to be fully matured to be open fractures. Lastly, open fractures were noted to dominate the boreholes in week four as compared to other durations. In this case, the borehole consisted of closed fractures with a great number of open fractures observed throughout. The rate at which the fracturing took place was very reasonable and allowed other mining activities to be fully completed around the rib

**Fig. 4** Borehole periscope observations on the development of extension fracture in **a** day, **b** week, **c** 2 weeks, **d** 3 weeks, **e** 4 weeks



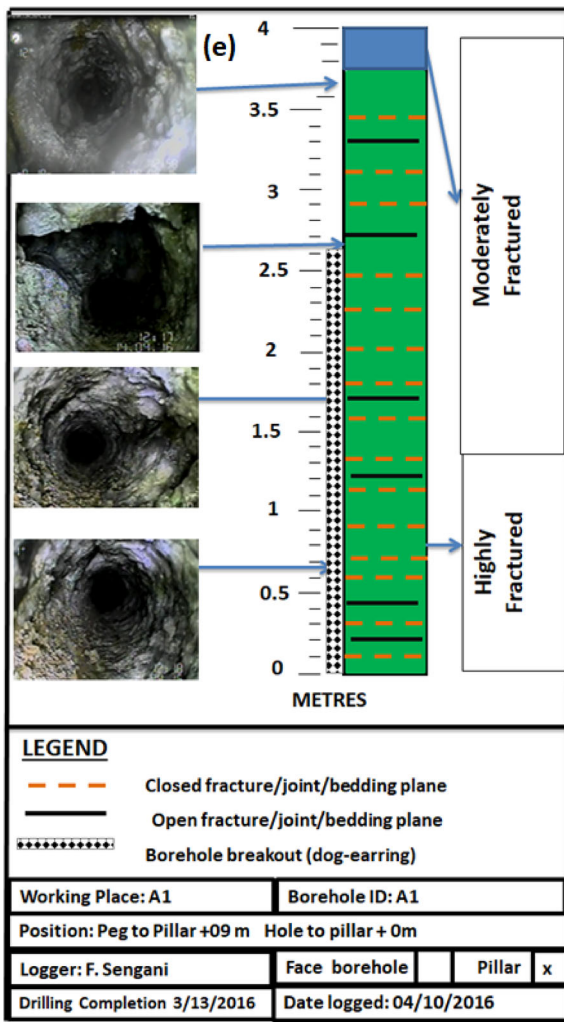


Fig. 4 continued

pillar and also allowed reasonable yieldability of the installed roof bolt to occur at a slower rate.

#### 4.1.2 Extension Fractures Initiation Heterogeneous Brittle Rib Pillars with Single Seismic Active Fault

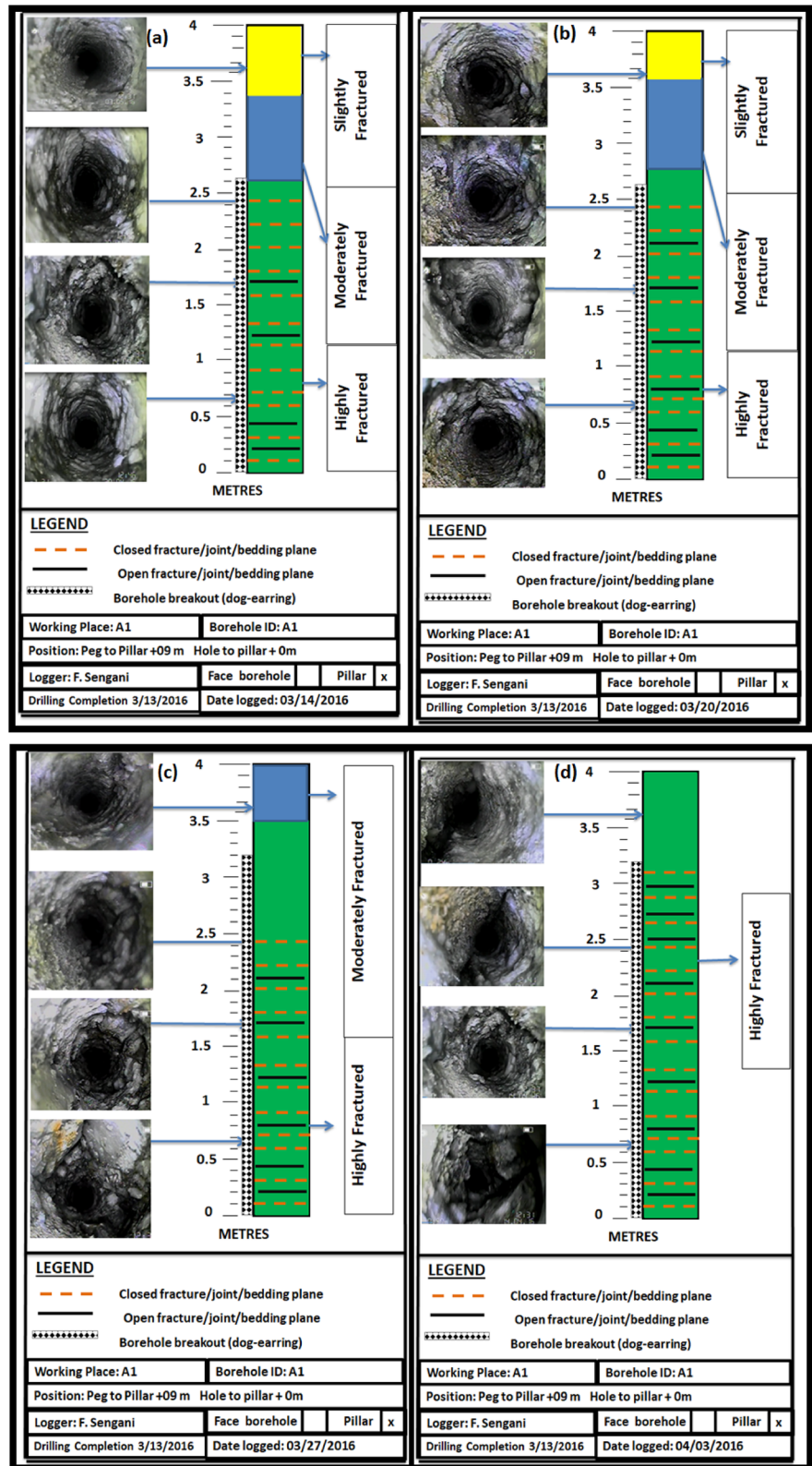
A similar investigation was conducted on a brittle rock pillar with single visible seismic active fault. The observation on the development of the extension fracture and extent were found to be moderately different from the first observation on a brittle homogenous rock pillar. It was noted that extensive fracturing was observed to extend to a depth of 1.5 m

after 24 h, followed by other zones like the homogenous brittle rock pillar in-stope pillar. However, the zone of extensive fracturing was noted to be dominated the boreholes after a 2 week. On the other hand, the solid zone noted within the first 24 h and the first week disappeared within 2–4 weeks. Like the brittle homogenous rock pillar, closed extension fractures were noted to become open fractures as time progressed (Fig. 4a–e). This result had a clear correspondence with Stacey’s extension criterion, in which the author (Stacey 1981) indicated that the “fracture of brittle rock will initiate when the total extension strain in the rock exceeds a critical value which is characteristic of that rock type”. This gives an impression that the composition of the rock mass plays a major role in the development of a fracture. Besides this study, studies by Borg and Maxwell (1956), Gallagher et al. (1974) and National Research Council (1996), indicate that the presence of geological features within the rock mass influences a regular development of fractures within the rock mass. Nevertheless, the initiations of extension fractures in this scenario were noted to be faster than the previous case study, thereby giving an impression that similar rock units with different compositions behave differently.

#### 4.1.3 Extension Fracture Initiations in a Heterogeneous Brittle Rock Pillar with Multiple Structures

Lastly, a heterogeneous brittle rock pillar with multiple faults was investigated where it was noted that the development of extension fractures was very different from the previous case studies. In this case study, boreholes were dominated with extensive fracturing, with the initiation of extension fractures taking place at an alarming rate as compared to another rock pillar. Extensive fracturing was noted from the boreholes collar to a maximum depth of 2.7 m on the first day of the investigation. In simple terms, a large portion of the boreholes was concentrated with extensive fracturing at the initial stage of the investigation. The rest of the boreholes consisted of moderate and slight fracturing (Fig. 5a). Furthermore, investigations after a week showed a rapid increase in the development of extension fractures toward the boreholes collar. Nevertheless, both moderate and slight fracturing were still noted after a week (Fig. 5b). After 2 weeks, a sudden disappearance of the slight fracturing zone was

**Fig. 5** Borehole periscope observations on the development of extension fracture in **a** day, **b** week, **c** 2 weeks, **d** 3 weeks, **e** 4 weeks



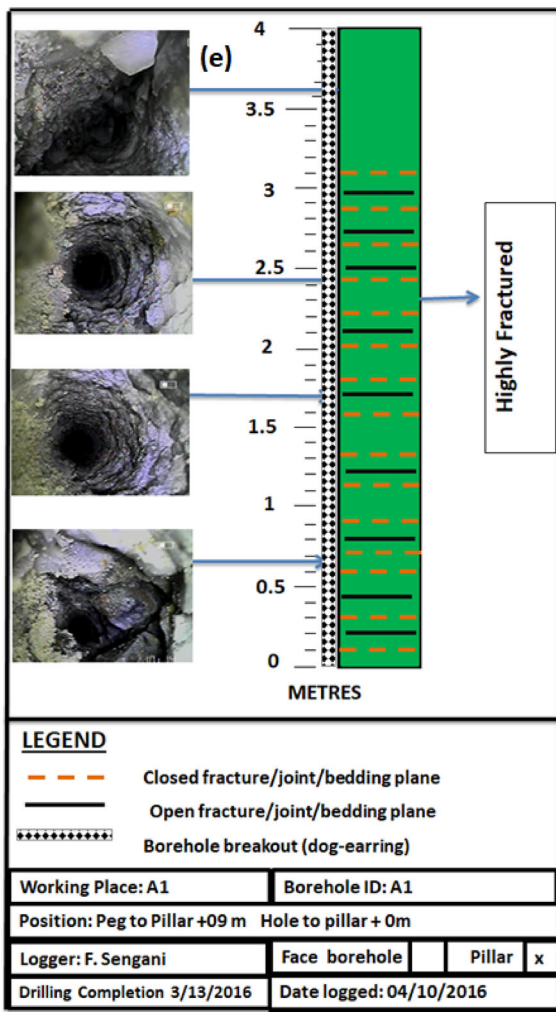


Fig. 5 continued

observed with a very small zone consisting of moderately fracturing rock mass, with a large zone of extensive fracturing (Fig. 5c). Three to four weeks later the borehole consisted of extensive fracturing throughout with open fractures dominating throughout the length of the boreholes (Fig. 5d and e).

From the observations above, it was noted that the development or initiations of extension fractures occurred with time. However, the initiation of extension fractures was noted to occur faster in a rib pillar composed of multiple seismic active faults. These results give an impression that rock mass properties contribute more on the rate in which extension fractures can be initiated. Nevertheless, it was also noted that extensive fracturing was generally noted from the borehole collar which gradually decreased as

it approached the rib pillar core in the first day of the investigations. Arguably, it can also be noted that the initiations of extension fractures were a time-dependent factor (time-dependant factor in a sense that they mature with time). Furthermore, the initiations of extension fractures were observed to be following a certain pattern in which close fractures were first developed because as time progressed the closed fractures became open fractures. These results give an impression that the initiation of extension fractures has different stages of maturity, which lead to a belief that extension fractures develop from micro-extension fractures to closed extension fractures and eventually to open extension fractures. All these phases take place as time progresses but the rate at which the process takes place is fully controlled by the rock mass properties (rock mass properties refer to the composition of the rock pillar, in which a rib pillar with multiple seismic active faults is expected to develop new extension fractures at a faster rate as compared to other rib pillar compositions) and magnitudes of the principal stresses acting on the rib pillars. As a result, it is believed that extension fractures mature with time and these results correspond well with other previous studies such as those conducted by Clotte et al. (1972–1973), Kuijpers (2000), van Aswegen and Stander (2012), Sengani and Zvarivadza (2018a).

#### 4.2 Ground Penetrating Radar

The understanding on the extent of extension fractures in a brittle homogenous and heterogeneous rock pillar was also evaluated using the Ground Penetrating Radar from all selected rock pillars. This was done with the purpose of comparing the results obtained from borehole periscope observations, with the GPR scans on the final day. From the scans, it was noted that extension fractures were evidenced to be developed differently from one brittle rock pillar to another. With the homogenous brittle rock pillar, the GPR scan showed extensive fracturing to occur within the first few metres toward the rib pillars core. Immediately after that zone, the rib pillars were dominated with moderate fracturing and then slight fracturing with very limited zones of less fracturing around the rib pillar core (Fig. 6a).

A further observation from the heterogeneous brittle rock pillar with single seismic active fault showed that extensive fracturing was noted to be

**Fig. 6** **a** GPR scan results on a homogenous brittle rock pillar, **b** with single seismic active fault, **c** with multiple seismic active faults. The bottom scan was conducted below the grade line (1.5 m from the footwall). The top scan was conducted above the grade line (above 1.5 m from the footwall). **d** Extension fractures initiations using GPR scan in a different composition of the brittle rock pillar

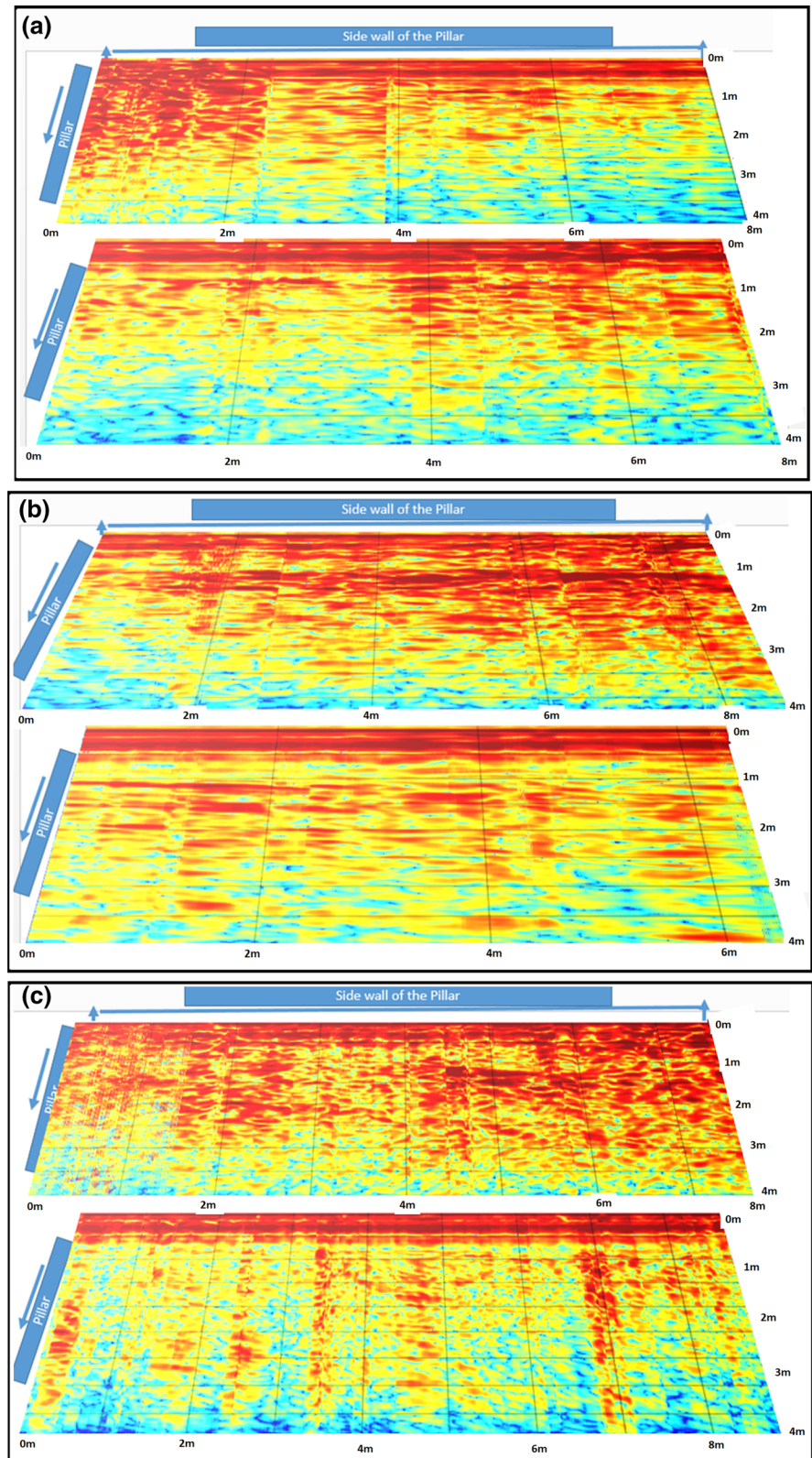
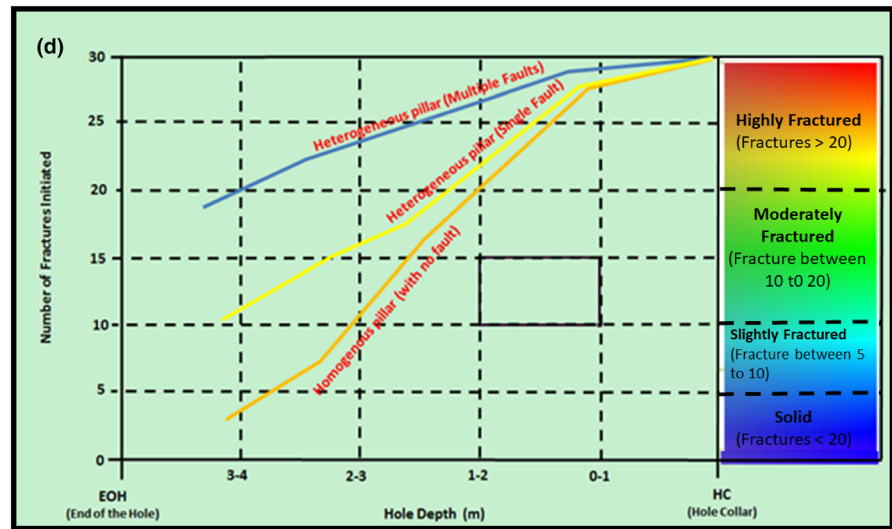


Fig. 6 continued



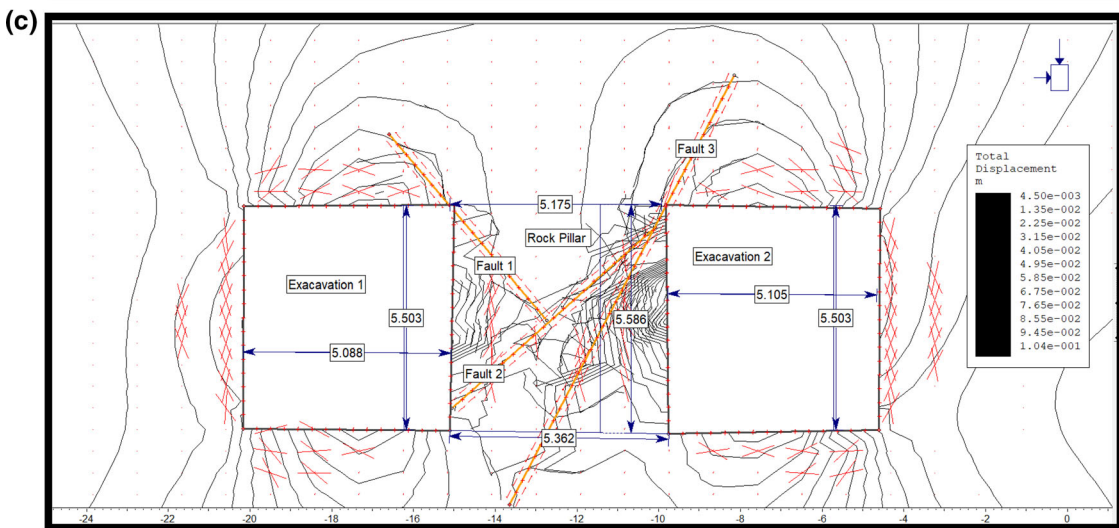
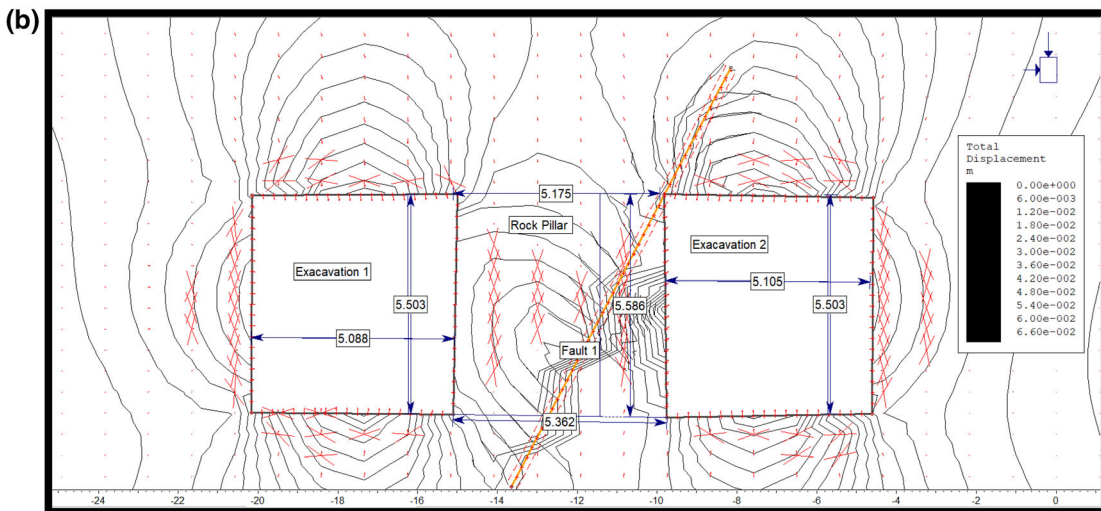
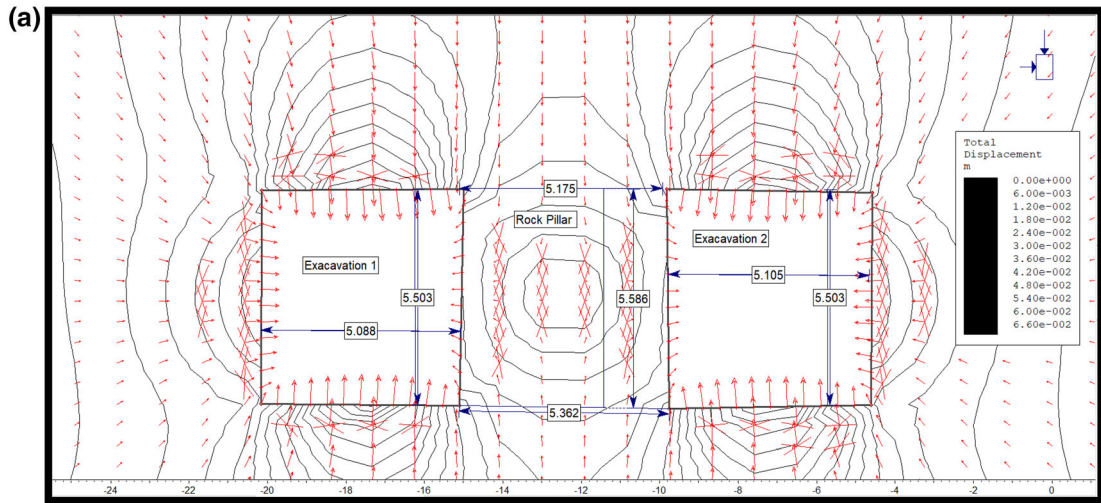
dominant for the large portion of the rib pillar, with small zones of moderate and slight fracturing taking place towards the rib pillar core (Fig. 6b). Lastly, the observation made from the heterogeneous brittle rock pillar with multiple seismic active faults showed extensive fracturing to occur throughout the rock pillar (Fig. 6c). In summary, the results of the three scans are presented on the graph shown as Fig. 6d. Figure 6d indicates the relationship between the depths of the rib pillar with fracturing relative to the composition of the brittle rock pillar. It can be observed from the graph that extensive fracturing was noted to take place throughout in the brittle rock pillar with multiple faults. The intensity of fracturing was observed to be gradually decreased with the composition of the rib pillars. As a result, this implies that the compositions of the brittle rock pillar indeed played a major role in the rate in which extension fractures were initiated within the rock pillar. Therefore, the results provide an impression that Stacey’s extension criterion (Stacey 1981) is related or can be related to the results but there are some few fundamental adjustments needed to align the criterion. The criterion seems to outline the behaviour of the homogenous brittle rock pillar with no visible seismic active geological features rather than the heterogeneous brittle rock pillar with single or multiple seismic active geological features. Therefore, this limitation has led into few suggested equations on how the criterion can accommodate the initiations of extension fractures at the different components of the

brittle rock pillars. Detailed results and discussions of suggested equations are presented below.

The curve in the blue colour represents the GPR scan results on a heterogeneous brittle rock pillar with multiple faults. The curve in the yellow colour represents the GPR scan results on a heterogeneous brittle rock pillar with a single fault and lastly, the orange curve represents a homogenous brittle rock pillar with no visible seismic active geological feature. These entire scans were conducted at the last week of the investigations which is week four. The purpose of doing that was to validate the results from the borehole periscope. Nevertheless, the GPR scan has little impact on identifying the fracture initiations due to its limitations, but it is one of the useful tools to validate empirical analysis (borehole periscope observations). The most common limitations associated with GPR scan poor performance due to high conductivity materials and signal are usually scattered in heterogamous material (Ryder and Jager 2002).

### 4.3 Rock Pillar Displacement Using Numerical Modelling

Rock pillar displacement associated with three composition of the rock pillar was also taken into consideration as to verify the results of the study. A simple numerical tool (EXAMINE 2D) was then used to simulate rock pillar displacement in three compositions as already outlined in the methodology. As already stated that this study present simple extension





◀ **Fig. 7** Rock pillar displacement **a** without any visible geological feature, **b** with single geological feature, **c** with multiple geological features

strain criteria, therefore simple numerical software was considered as to validate the results of the study, however complex numerical software were not appropriate at this initial stage of the development of the criteria but they will be considered in future. Nonetheless, the results of the simulation have shown little or less rock displacement to occur in a rock pillar that has no visible geological feature. This results were concluded based on the spacing on the contours along the rock pillar. Secondly, gradually increase on the rate of rock pillar displacement was noted when the rock pillar was composed of single geological features and lastly extensive rock pillar displacement was noted when the rock pillar was composed of multiple geological features. The results are clear shown in Fig. 7a–c.

This kind of behaviour have been evidence in several studies such as Andrews and Sengani (2017), Zvarivadza and Sengani (2018b). Andrews and Sengani (2017) have presented some of the encouraging results on pillar behaviour, in which the authors reported that the bottom and top part of the rock pillar are usually expected to be solid while the middle portion of the pillar is expected to undergo extensive scaling as a results of extensive fracturing taking place, which can either due to geological feature or stress levels subjected to the rock pillar or inappropriate rock pillar design. Zvarivadza and Sengani (2018b) also presented encouraging results in which the authors have evaluated rock pillar failure based on the composition of the pillar and design of the pillar. It was noted that geological features contribute largely on rock pillar failure in which most of the pillar failure were associated with extensive fracturing and scaling. Nevertheless, the results from the above authors correspond very well with simulated results, in which a rock pillar with no geological feature is expected to perform well as compared to the other two group.

#### 4.4 Criteria for Extension Fractures Initiations

The understanding on the initiations of extension fracture has gained much more interest from the past, but currently, there are many complex methods used to

estimate initiations of extension fractures within a rock mass at the vicinity of underground excavations. However, most of the complex methods/conventional hypothesis (Griffith and Mohr criteria) have been reported to be inadequate to estimate the initiations extension fracture (Clausing 1959; Handin et al. 1967; Stacey 1981; Wesseloo and Stacey 2016). As a matter of fact, Stacey's extension strain criterion is reported to be one of the simplest appropriate hypothesis to estimate the initiations of extension fractures (Waldeck 1979; Stacey 1982, 1989; Stacey and Harte 1989; Pang and Goldsmith 1990; Stacey et al. 2003; Ndlovu 2006; Ndlovu and Stacey 2007; Steffanizzi et al. 2007; Andersson et al. 2009; Nicksiar and Martin 2012; Li and Wong 2013; Wesseloo and Stacey 2016; Sengani and Zvarivadza 2018c). Nevertheless, minor limitations were noted from Stacey's extension criterion (Stacey 1981), firstly, an appropriate rate in which extension fractures are expected to be initiated from different rock mass composition is not established, secondly, there is no known empirical studies on the prediction of extension fractures at high stress environment. Therefore, a detailed study was conducted which improved equations from Stacey Extension strain creation (Stacey 1981) as suggested below.

There are three equations suggested in this study that clearly present how extension fractures are developed in a different composition of a brittle rock pillar in high stressed ground conditions. The results of the study have shown that the rate at which a fracture is initiated when a rib pillar is composed of no visible seismic active geological features differs from a brittle rock pillar with single or multiple seismic active geological features. Therefore, Eq. 3 presents the initiations of extension strain in a homogenous brittle rock pillar (rock pillar without any seismic active geological feature) minor strains with an additional factor ( $f_n$ -for homogenous brittle rock pillar). Equation 4 presents the initiations of extension strain in a brittle rock pillar with single seismic active fault, with an additional factor ( $f_s$ -for heterogeneous single seismic active fault) while Eq. 5 presents the initiation of extension strain in a brittle rock pillar with multiple seismic active faults ( $f_m$ -for heterogeneous single seismic active fault). The factors  $f_n$ ,  $f_s$  and  $f_m$  are constant values which are calculated using the ratio of a total number of extension fractures counted within one portion of the boreholes. In actual sense, the extension fractures that occurred from 1 to 2 m in day

one were compared in all conditions with the rib pillars, the zone was selected because it was less affected by blasting shocks and a brittle homogenous rock pillar was used as a baseline both for the brittle heterogeneous rock pillar with a single fault and that with multiple seismic active faults. The constant values obtained are as follows; 1 for  $f_n$ , 0.85 for  $f_s$  and 0.65 for  $f_m$ .

$$\varepsilon_3 = \frac{1}{E} [[\sigma_3 - \nu(\sigma_1 + \sigma_2)] \times f_n] \quad (3)$$

$$\varepsilon_3 = \frac{1}{E} [[\sigma_3 - \nu(\sigma_1 + \sigma_2)] \times f_s] \quad (4)$$

$$\varepsilon_3 = \frac{1}{E} [[\sigma_3 - \nu(\sigma_1 + \sigma_2)] \times f_m] \quad (5)$$

where  $\sigma_1$ ,  $\sigma_2$ ,  $\sigma_3$  are the principal stresses,  $E$  is the modulus of elasticity,  $\nu$  is Poisson's ration,  $f_n$  is the factor used for a brittle rock pillar without any visible seismic active geological feature,  $f_s$  is the factor used for a brittle rock pillar with single visible seismic active fault and  $f_m$  is the factor used for a brittle rock pillar with multiple visible seismic active faults.

Similar to the suggestion made by Stacey's extension criterion (Stacey 1981), the extension strain occurs when  $\nu(\sigma_1 + \sigma_2) > \sigma_3$ . In this study, it was noted that the extension fractures could be initiated at very low extension strain depending on the composition of the rock mass. As a result, it was found that in the case of a brittle in-stope pillar with no features or seismic active geological feature, extension fractures occurred as per Stacey's Extension Strain criterion. Furthermore, the analysis shows that the extension fracture turns to occur at a very low strain in a brittle heterogeneous rib pillar composed of a single visible seismic active geological feature as compared to the homogenous brittle rib pillar. In actual sense, an extension strain occurred at a ratio of 1:0.85 compared to the homogenous brittle rib pillar. As such, it has been clearly observed that the brittle heterogeneous rib pillar with a single seismic active fault was heavily fractured or heavily disintegrated, meaning that a slight movement allowed the initiations of extension fractures which was the opposite case in the homogenous brittle rib pillar.

In the case of the heterogeneous brittle rib pillar with multiple seismic active faults, the initiation of fractures took place at an extremely low strain. A ratio of 1: 0.65 was obtained; this clearly means that initiation of extension fractures is expected to occur at an extremely low extension strain due to multiple faults which further disintegrate the rock mass. In this case, a minor strain has the possibility to initiate extension fractures. Therefore, the equations above illustrate that extension fractures are formed at a different rate based on the composition of the brittle rib pillars. However, the initiations of the extension fractures still follow the initial concept of extension fracture initiations by Stacey (1981). Nonetheless, this study has suggested new inputs which incorporate the rate at which extension fractures are initiated. This leads to a modified Stacey's extension criterion, in which it is believed that extension fractures are initiated when  $(\nu(\sigma_1 + \sigma_2) > \sigma_3) \times f_n$ , for a homogenous brittle rib pillar, also initiated  $(\nu(\sigma_1 + \sigma_2) > \sigma_3) \times f_s$ , for a heterogeneous brittle rib pillar with single seismic active fault and lastly  $(\nu(\sigma_1 + \sigma_2) > \sigma_3) \times f_m$ , for a heterogeneous brittle rib pillar.

It is also crucial to indicate that the suggested equations illustrate that extension fractures can be formed when all three principal stresses are compressive as well as when the net macro stress is compressive. Owing to that, after the extension fracture has formed the macro across the fracture has the possibility to remain compressive but there are several factors contributing to that. One of the factors is the behaviour of the three principal stresses. The principal stresses have the major control on the occurrence of strains within the rock mass, therefore their interaction is imperative. These equations can easily simplify the occurrence of extension fractures within a different type of brittle rock pillar and eliminate the use of complex and sophisticated methods on fracture initiations. Suppose a critical extension strain at fracture initiation determined from a brittle homogenous rock pillar ranges from 0.000073 to 0.000086 (as per Stacey 1981, Table 1), it therefore means that for a brittle homogenous rock pillar with single seismic fault, a critical extension strain at fracture initiation would be expected to range from 0.000062 to 0.000073. In the case of a brittle heterogeneous rock pillar with

multiple seismic active faults, a range of 0.000047–0.000055 is expected. This gives an impression that an extension fracture is expected to be initiated at extremely low extension strain in a heterogeneous rock pillar with multiple features as compared to a homogenous brittle rock pillar. This corresponds well with the observations reported by several authors, Borg and Maxwell (1956), Gallagher et al. (1974), and the National Research Council (1996) which indicated that the heterogeneity and textures in rocks have the ability to cause pervasive heterogeneities in the stress field. As a result, the presence of geological features were found to contribute much on the initiations of fractures in the rock mass.

Furthermore, Lawn and Wilshaw (1975) also indicated that in a situation of linear elastic fracture mechanics, a fracture is expected to propagate when the stress intensity factor exceeds a critical stress intensity factor or fracture toughness, however, this condition is assumed to be controlled by material property. Further studies by Brace et al. (1966), Scholz (1968), Peng and Johnson (1972), Hallbauer et al. (1973) and Martin and Chandler (1994), have shown that the initiation of fractures in uniaxial laboratory tests takes place between 0.25 and 0.5  $\sigma_c$  which also supports the suggestion made by Stacey (1981). Stacey (1981) conducted laboratory tests on different rock types and found out that in most brittle rocks, the critical strain for extension fracturing was slightly dependent on confining stress (Cai et al. 1998) and largely dependent on the characteristic of the rock type involved. Stacey (1981) concluded that the initiations of extension fractures takes place in the region of 0.3  $\sigma_c$  (Cai et al. 1998). Nevertheless, the suggested equations seem to agree with relevant studies in the field of study, although the equations suggested the rate in which the extension fractures occur in different brittle rock pillars. Brace and Byerlee (1968) conducted an experiment of a brittle rock fracturing where the authors found out that dilation associated with fracture began at a stress of one-third to two-thirds of the ultimate fracture strength. Rummel (1971) indicated that primary ‘tensile’ crack initiation takes place at about one-third of the ultimate strength. These last two studies give an impression that the initiations of fracture always differ from one rock type to another based on the composition in which the rock consists of.

Therefore, the rate at which a fracture is initiated will depend totally on the composition of the rock mass.

#### 4.5 Time-Dependent Chart of Extension Fracture Initiations

This section presents a simple time-dependent chart of extension fracture initiations developed based on the observed behaviour of different compositions of the brittle rock pillar in high-stress ground conditions. Using borehole periscope observations, it was possible to come up with a meaningful chart that describes extension fracture initiations in time to time. There are three charts developed which differ based on the composition of the rib pillar. In simple terms, the above-suggested Eqs. 1–3 are the representations of the three charts.

The first chart represents the initiations of extension fractures in a brittle rock pillar without any visible seismic active fault (Fig. 8a). The chart is based on high stress at the depths ranging from 2500 to 4500 m from the earth surface in South African hard rock mining. The chart simplifies the understanding of how extension fracture initiations can be estimated. Therefore, in simple terms, the first chart shows that the first few metres of the brittle rock pillar are expected to be highly fractured and consist of several fractures greater than 20 in a day after the rib pillar is fully constructed. Furthermore, the chart also shows that as the depth of the borehole increases the intensity of extension fractures gradually get reduced to a point where the solid zone is encountered toward the rock pillar core with fractures of less than 5. In the first week, it was expected that the first few meters (from pillar collar to a maximum of 1.2 m) would experience high fracturing, followed by moderate fracture from 1.2 to a maximum depth of 1.9. Slight fracturing was also expected from 1.9 m to the maximum depth of 2.3 m meanwhile very low fracturing was observed at 2.4 m solid zone to the rib pillar core.

After 2 weeks the initiations of extension fractures was expected to increase gradually, wherein the chart clearly shows that the development of a new extension fracture was expected to rapidly increase to a maximum depth of 3 m with few initiations of extension fractures from 3 m to the pillar core. On the other hand, in week four extensive development of extension fracturing was expected wherein the initiations of extension fractures was expected to occur to a

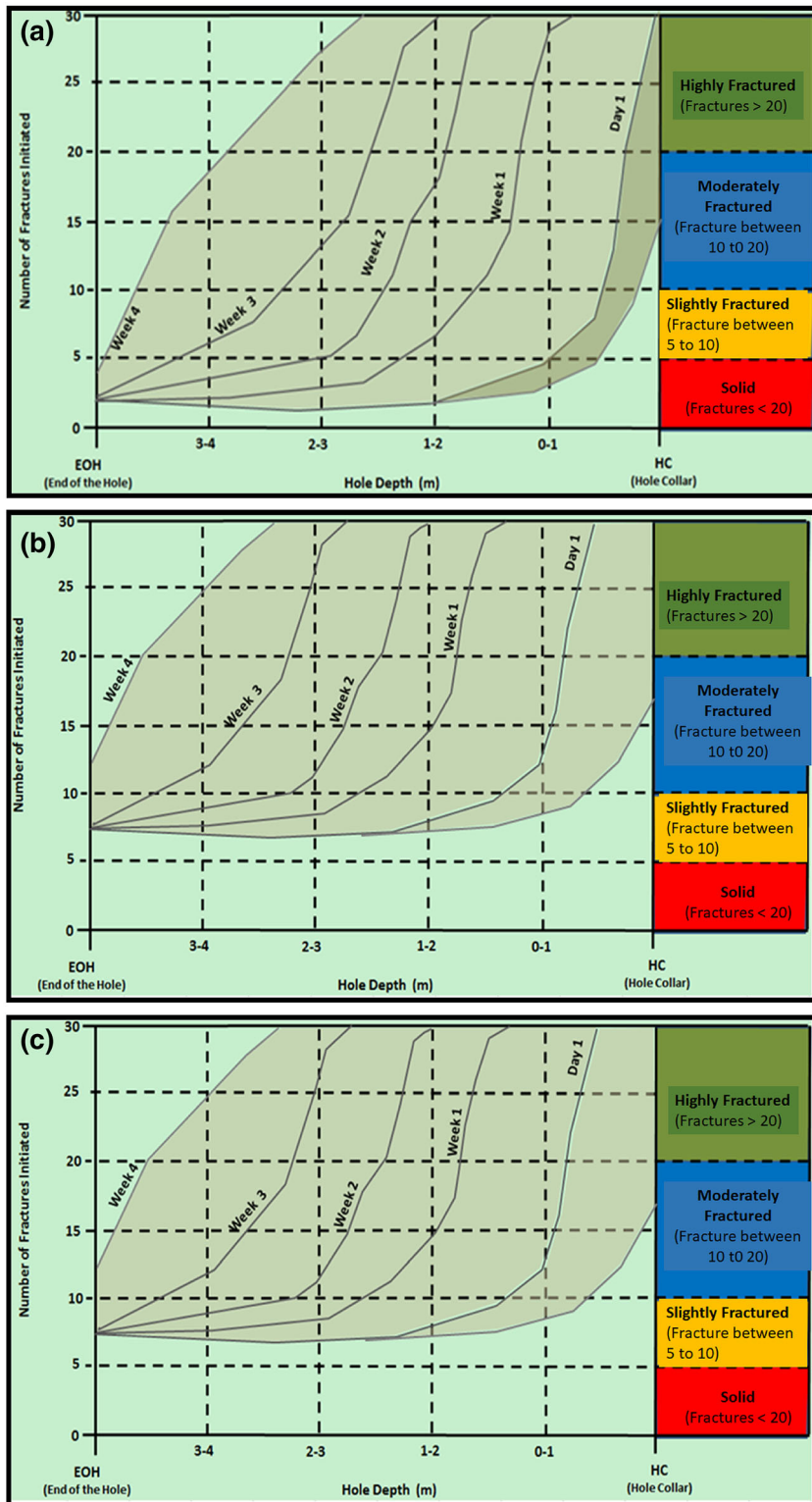


**Fig. 8** Time-dependent chart of fracture initiations on a brittle homogeneous rib pillar **a** with no seismic active faults, **b** with single seismic active faults, **c** with multiple seismic active faults

maximum depth of 3.5 m. At this stage a brittle rock pillar is expected to be dominated with extensive fracturing and limited zones of moderate to slight fracturing. The results expected by the chart in week four usually represent a rib pillar which has yielded and this gives an impression that a rib pillar is expected to be fully yielded after 4 weeks of fully constructed (rock pillar construction) provided the conditions are favourable. In summary, the first chart presents the expected initiations of extension fractures in a homogenous brittle rib pillar at the high-stress environment. From the chart, it can be deduced that the initiations of extension fractures occur time to time and the development of fractures is mostly controlled by the rock mass properties together with magnitudes of principal stresses acting on the rib pillar.

The second chart represents the initiations of extension fractures of a brittle heterogeneous rock pillar with a single visible seismic active geological feature (Fig. 8b). The chart shows that in day one, the first-meter and half of the boreholes are expected to experience extensive fracturing, thereafter moderately, slightly and followed by solid zones of fracturing respectively. In simple terms, extension fractures are expected to be initiated at a greater rate as compared to the first chart. After a week, the chart indicates that rapid initiations of extension fracturing were expected to a maximum depth of 2.8 m and then gradually decrease from 2.8 m to the rock pillar core. From week two to week four, the chart represents a rapid increase in the initiations of the extension fracture for every metre. In week four, a small portion of the rib pillar is expected to consist of slight fracturing which occurs very closely to the rib pillar core and within the core. On the other hand, the rest of the borehole from the pillar collar to the maximum depth of 3.8 is expected to be dominated with extensive fracturing. In this scenario, a rib pillar is expected to be fully yielded in 3 weeks rather than 4 weeks as compared to the brittle homogenous rib pillar. This gives the impression that the yield ability of the rib pillar is also controlled by the composition of the rib pillar. Nevertheless, this chart also gives an impression that if the chart is not supported after 3 weeks, therefore, the installation of the support system will not be as effective as expected because the

drilling and installation process will be a very difficult activity. As a matter of fact, this chart can also be used as a robot rating system in which one can predict the yieldability and support effectiveness based on the depth of fracturing within the rib pillar.

The last chart presents the initiations of extension fractures in a brittle heterogeneous rock pillar with multiple visible seismic active faults (Fig. 8c). This chart usually presents the most common behaviour of brittle rock pillars in highly stressed ground conditions. Nevertheless, the chart indicates that in day one, the borehole is expected to be dominated with highly fractured zones and moderately fractured zones from the borehole collar to a maximum depth of 1.4 m. From 1.4 m to the pillar core slight fracturing is expected. The chart indicates that more than 20 extension fractures were expected to be initiated from the borehole collar to a maximum depth of 1.4 m. It also indicates that the ground conditions were heavily fractured in which the initiation of new extension fractures do not require large strain. Nevertheless, from week one to week four, the brittle rock pillar is expected to be dominated by high and moderate fracturing toward the pillar core. In this case, the initiation of the extension fracture is at a rate of 0.65 to the homogenous brittle rock pillar. However, to explain the initiation of the extension fracture in this chart, the initiation of the extension fracture takes place at extremely low extension strain, meaning that the rock mass strength of the rock mass is extremely reduced by the presence of multiple seismic active faults. As a result, the initiations of extension fractures requires very low extension strain to generate extension fractures. These types of rib pillars are expected to encounter their yielding point at the early stage after the rib pillar is fully constructed. In simple terms, 2–3 weeks after full construction of the rib pillar, the rib pillar is expected to be fully yielded. As a matter of fact, if the installation of the support system is delayed, the rib pillar is expected to be scaled-down or mine itself and eventually it will collapse because there will be nothing holding the small rocks together. From an observational point of view in underground situations, such a rib pillar is usually noted by extensive bulking on both sides of the rib pillar. However, after the rib pillar has reached a yielding point, it relaxes or remains stable.

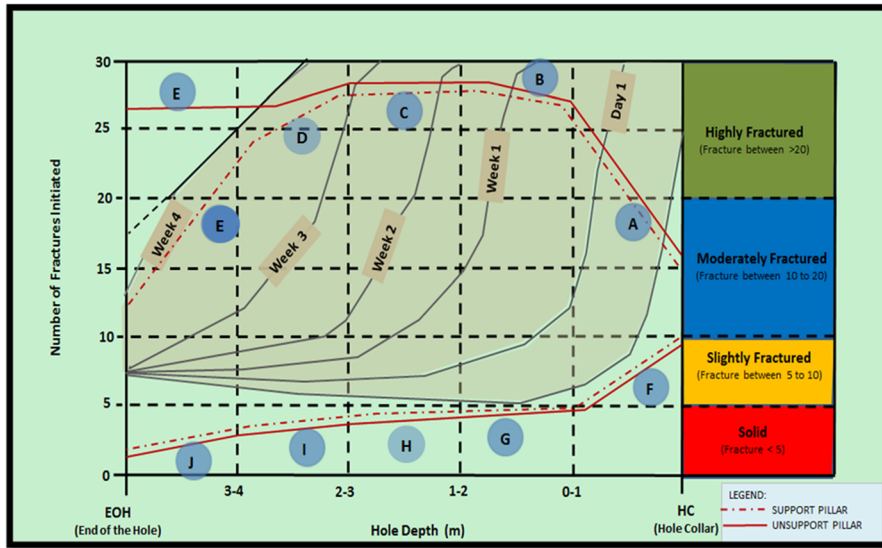


**Fig. 9** Estimation of rock pillar behaviour using the extension fracture initiations chart

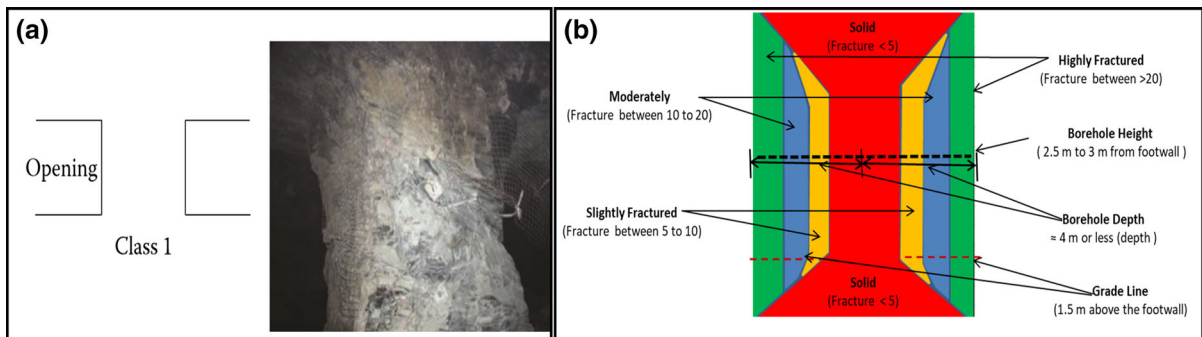


**Fig. 10** **a** Reproduction of Fig. 5.44 of Villaescusa (2014) as a Schematic illustration of the pillar stability classification method developed for use at Westmin Resources Ltd. (after Lunder 1994, 166 pp.), **b** rib pillar with slight yielding behaviour

4.6 Application of the Charts

The charts and criterion developed are simple to use in a practical manner and are not too complex. The criterion is an improved Stacey Extension criterion and only differs because it is an improved criterion that can differentiate the initiation of extension fractures in different brittle rib pillars while the Stacey Extension Criterion generalized the initiations of extension fractures. It is not expected that the chart will be applicable in all rock types as well as at any stress levels. Therefore, it is crucial to indicate that sophisticated methods are required to further the study and other studies in different rock types and stress levels. Two examples are presented in which the first example

is on the estimation of rib pillar stability and the second example is on the estimation of support installation quality.

4.6.1 Estimation of Rib Pillar Stability Using the Chart

Pillar design and stability analysis are critical components of the mine design process (Villaescusa 2014). The factor of safety using the pillar strength/average pillar stress ratio is extensively established as a tool that is now popular as it allows more quantitative analysis (Villaescusa 2014). In rock mechanics, the term stability mostly refers to the stability of equilibrium (Salamon 1970; Brady and Brown 2004). In the

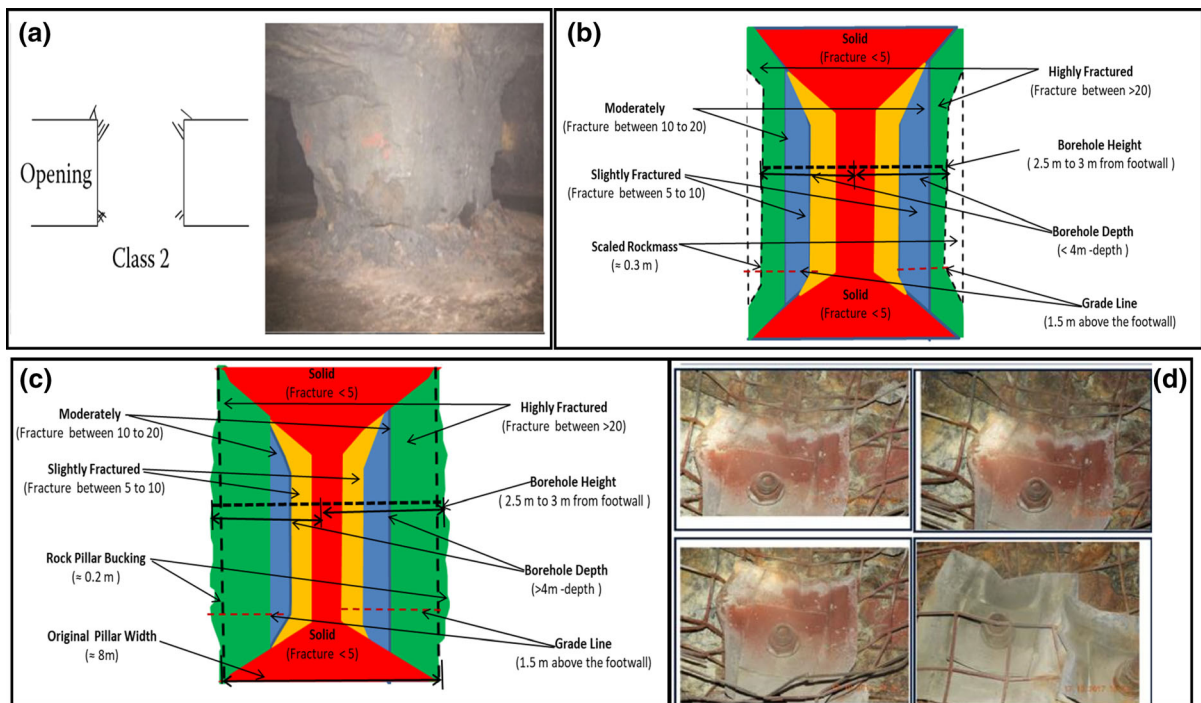


**Fig. 11** **a** Reproduction of Fig. 5.44 of Villaescusa (2014) as a Schematic illustration of the pillar stability classification method developed for use at Westmin Resources Ltd. (after Lunder 1994, 166 pp.), **b** rib pillar with moderately yielding

behaviour, **c** rib pillar with moderately yielding behaviour and bulking on the sidewall of the pillar and **d** reproduction of Fig. 22 of Sengani (2018a, b) as being the performance of Garford bolts in a seismic event

past, the stability of rib pillars has been excluded from the design system, as a result Hoek and Brown (1980), have proposed an equation that explains the stability of rib pillars using the equivalent area method. A few decades later there were extensive studies (Hedley and Grant 1972; Von Kimmelman et al. 1984; Krauland and Soder 1987; Hudyma 1988; Sjöberg 1992; Lunder 1994; Lunder and Pakalnis 1997) on validating the suggestions made by Hoek and Brown (1980). Lunder (1994) proposed an empirical criterion on estimating the stability of rib pillars based on classes, and this proposed criterion was accepted by many scholars. In this study, a simple criterion using the proposed chart to determine the stability of the rib pillars based on fracture frequency is suggested. The estimation of rib pillar stability is described in the chart below. The chart has red dotted lines which indicate supported rib pillars while the solid red line represents un-supported rib pillar. The stability of the rib pillar is expressed using alphabets from A to J (Fig. 9).

Based on the underground observations and periscope observations, at point A both rib pillars

(supported and unsupported) usually experience their initial stage of slight yielding with moderate fracturing on the average pillar width (Fig. 10a). The pillar is mostly composed of extensive fracturing from the pillar collar to few metres within the pillar followed by moderate, slight and the solid zones respectively (Fig. 10b). This kind of behaviour has been evidenced in many studies such as Lunder (1994) in which the author calls this behaviour class 1 (Fig. 10a). The author indicated that the rib pillar is expected to have no sign of stress-induced fracturing based on the observational point of view. Indeed, on the observational point of view, the rib pillar resembles no sign of induced fracturing or extension fracturing but if one conducts borehole periscope to see the morphology of fracturing within the rib pillar at that stage, then few extension fractures are observed to have developed with extensive fracturing from the borehole collar to few metres from the borehole collar. Therefore, this study simplifies and provides more detail on how the rib pillar is expected in a class 1 category as per

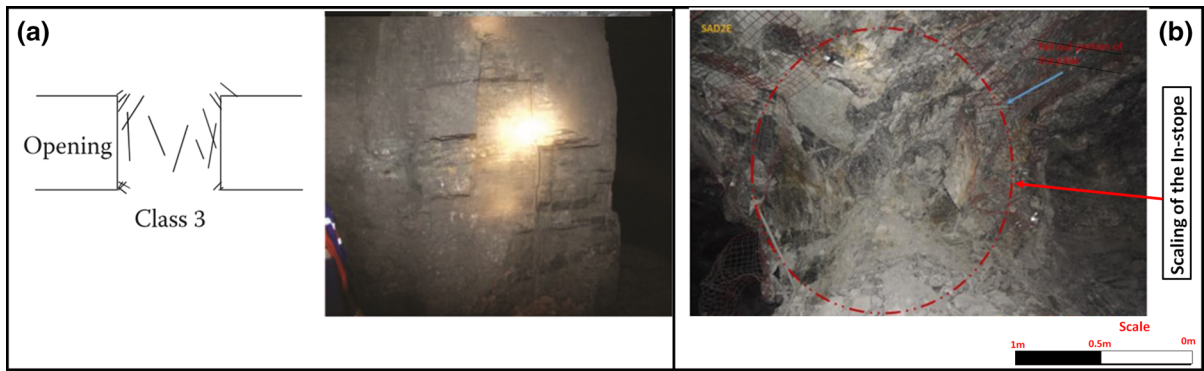


**Fig. 12** a Reproduction of Fig. 5.44 of Villaescusa (2014) as a Schematic illustration of the pillar stability classification method developed for use at Westmin Resources Ltd. (after

Lunder 1994, 166 pp.) and b modified Fig. 5 of Zvarivadza et al. (2017), being in-stope Pillar fracturing and scaling

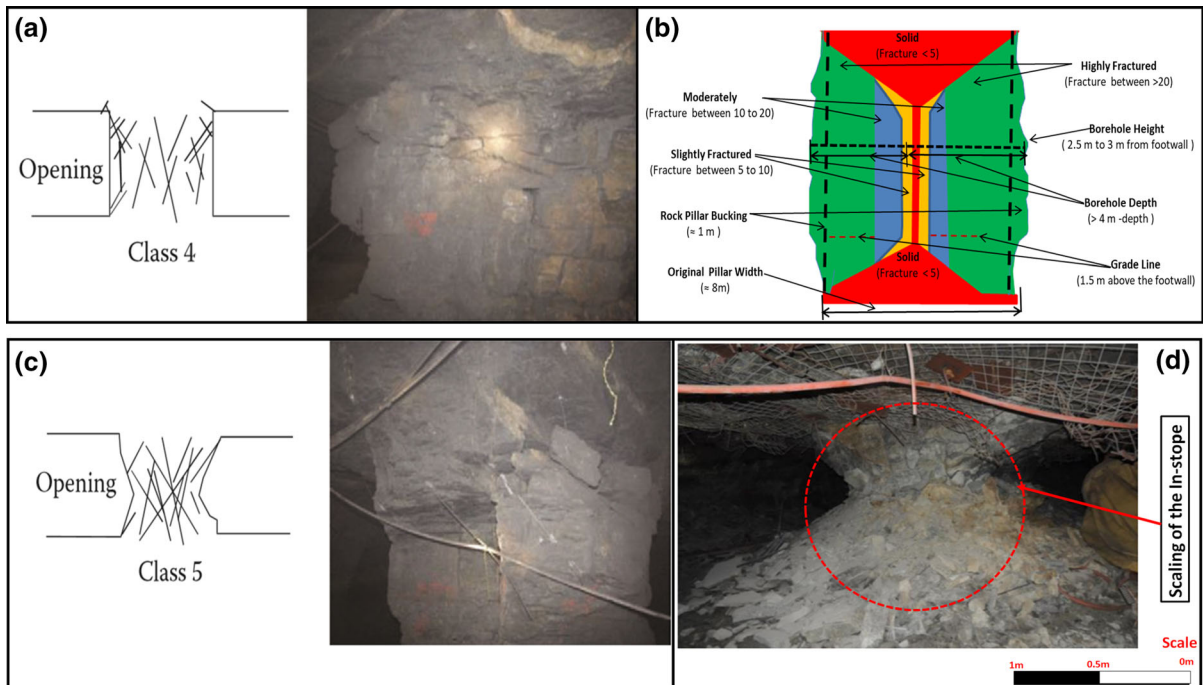


**Fig. 13** a Reproduction of Fig. 5.44 of Villaescusa (2014) as a Schematic illustration of the pillar stability classification method developed for use at Westmin Resources Ltd. (after Lunder, 1994, 166 pp.), b rib pillar which is fully yielding. c Reproduction of Fig. 5.44 of Villaescusa (2014) as a

Schematic illustration of the pillar stability classification method developed for use at Westmin Resources Ltd. (after Lunder, 1994, 166 pp.) and d modified Fig. 6 of Zvarivadza et al. (2017) being in-stope pillar with extensive scaling

Lunder (1994) which corresponds with category A or point A in the chart.

Point B, represents the moderately yielding of the rib pillar and at this stage the majority of the pillars consist of minor scaling taking place along the corner of the rib pillar (Fig. 11a), while the fracture

frequency still follows the pattern of heavy fracturing from the pillar collar to a few metres, followed by moderate, slight and solid zone (Fig. 11b). On the other hand, if the rib pillar is supported, minor bulking with few small broken rocks contained within the welded mesh is expected (Fig. 11c). From an



observational point of view, in deep-level gold mines South Africa, the support system such as Garford hybrid bold shows some early stage of yielding (Sengani 2018a, b). The plate and bolts show little deformation to take place (Fig. 11d).

At Point C, most of the observed rib pillars are fully yielded at this stage, and usually fully fractured with a small portion of the pillar core being moderately fractured. According to Lunder (1994), fracturing in pillar walls, fractures < half pillar height in length and fracture aperture < 5 mm are expected (Fig. 12a). As already mentioned that Lunder (1994) did not further the understanding on how fractures are developed within a pillar, nevertheless his observation corresponds to the actual observation made in this study. As such, observations related to class 3 of Lunder (1994) have been reported by Zvarivadza et al. (2017) in which the rib pillar resembles pillar scaling and extensive fracturing from the first few meters (Fig. 12b).

Point D represents a yielded rib pillar comprised of the disintegrated rock mass that is held together with a support system and at this stage the rib pillar is not expected to burst or crushed since it is fully yielded and supported (Fig. 13b). However, if support systems can be stripped the rib pillar can be completely mined itself (Fig. 13c). According to Lunder (1994), a rib pillar will represent fractures > half pillar height in length and fracture aperture > 5 mm, < 10 mm (Fig. 13a). Due to the fact that the rib pillar is extensively fractured, minor disturbance in the rock mass can lead to rapid scaling on both sides of the rib pillar. Point E represents a rib pillar which is not supported or fully supported; at this stage, a rib pillar is expected to collapse due to the fact that the pillar has already fully fractured with small rocks that are not held together by an adequate support system (Fig. 13d). Figure 13d represents the disintegration of the pillar, blocks falling out from pillar, fracture aperture > 10 mm and fractures through pillar core (Lunder 1994).

At points F to J, a rib pillar either supported or not, is expected to experience less fracturing with the possibility of building up stress. Due to such composition, a rib pillar is then expected to burst or experience extensive bulking on both sidewalls of the pillar. This conditions usually happen when a large pillar is used rather than a normal pillar that is suitable for the design. From the few examples on how

the chart can be used to estimate the rib pillar stability, the chart corresponds very well with previous studies such as Lunder (1994), Villaescusa (2014), Sengani and Zvarivadza (2017) and others. Nevertheless, the chart seems so simple to utilise and it combines both the observational point of view as well as borehole periscope observation. Therefore, the two analyses correlate well.

#### 4.6.2 Estimation of Support Installation Quality Using the Chart

The quality of the support system is always crucial in both surface and underground excavations. The charts can also be used to determine the quality of support installation as time progresses for different types of brittle rock pillars. Louchnikov (2011) conducted a study in a long hole stoping mining operation, using the extension strain criterion to predict fracturing around stopes with the purpose of designing an appropriate rock support system. As a result, the study has used the extent of fracturing to successfully identify the appropriate support system required for the stopes. Prior to that, this study also finds it crucial to propose a chart that can be used to predict the depth of fracturing in designing an appropriate support system in different excavations. Figure 14 presents an extension fracture initiations chart for a brittle heterogeneous rock pillar with multiple seismic active geological features. The chart is then composed of points A to D, with each point having its meaning in this chart.

At point A, the ground conditions are expected to be moderately fractured and during this duration the installation of support systems can be properly done, whereas drilling can be conducted smoothly. In actual sense, drill steal is not expected to stack along the rock pillar since the pillar is moderately fractured. A good example was reported by Zvarivadza and Sengani (2018a) on the performance of a yielding support system in deep-level gold mines (Fig. 15a).

At point B, the conditions of the rock pillar are highly fractured, where the drill of a single hole can take longer than the expected time, because the drilling steel will be stuck throughout. In actual sense, when drilling a brittle rock pillar which has reached its fully yielding stage, it is very difficult to install the required support system in a reasonable time, as a result several drill steels are used (Sengani and Kataka

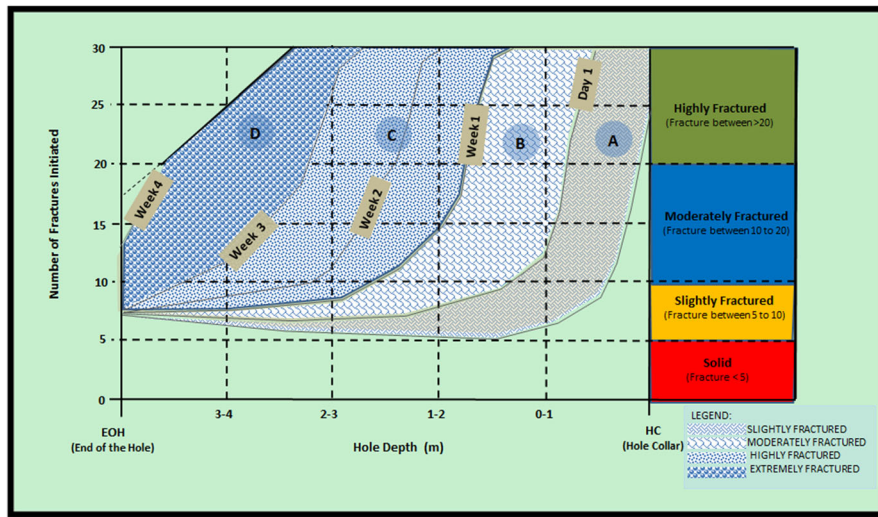


**Fig. 14** Estimation of support installation quality using the extension fracture chart

2017). Sengani and Kataka (2017) compared the performance of a standard drill rig and a roof bolter on support installation. Their study has indicated that when drilling a brittle rock mass in which the pillar has already yielded, it becomes very difficult to complete support installation as per estimated duration. As a result, it is advisable that support installation be undertaken before the estimated duration expires. It is also advisable that in order to save the cost of mining and to improve the safety of the employees, support installation should be conducted immediately after blasting. Figure 15b represents a pillar with a roof that is poorly installed due to extensive fracturing taking place within the rib pillar. In actual sense, the support

system could not be done properly because it was very difficult to achieve full length drilled boreholes for support installation because some of the boreholes closed immediately after drilling.

Lastly, from point C to D, the rock pillars are extensively fractured and drilling such types of pillar usually leads to self-mining of the in-stope pillar. In simple terms, if support installation is proposed to be undertaken after 2 weeks, it is expected that the pillar can be scaled out to the core depending on the extent of fracturing at that time. From the above discussion, the chart is so simple to implement and can improve the standard of safety within the deep level mining houses and other mines. It is crucial to indicate that this

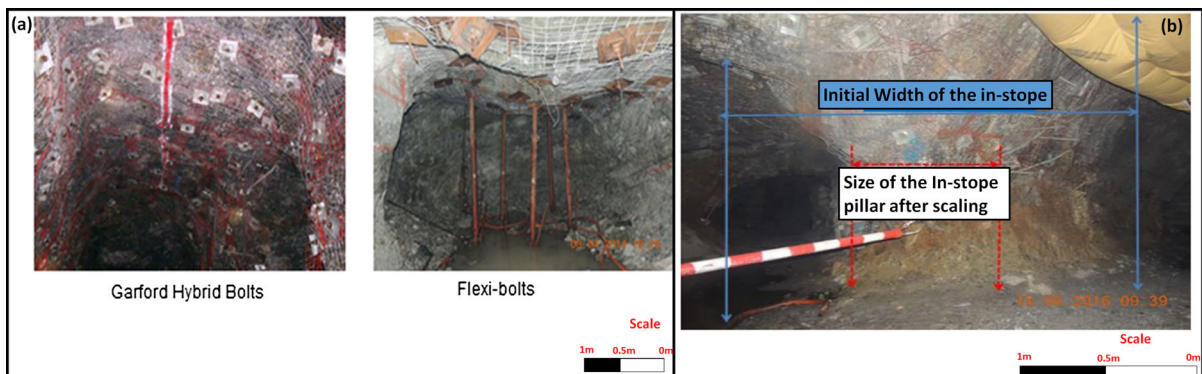


**Fig. 15** a Reproduction of Fig. 17 of Sengani and Zvarivadza (2018b), being the performance of yielding bolts under dynamic movement (seismic events), and b reproduction of Fig. 3 of Zvarivadza et al. (2017), being in-stope pillar scaling

chart does not include any sophisticated methods thereby requiring that many sophisticated methods be used and be compared with this chart. In addition, this chart is not expected to solve all the problems in every mine but rather to address some problems where it is applicable and necessary.

In supporting the applicability of the chart, a recent book on “*Rockburst Support*” by Cai and Kaiser (2018) has reported one of the fundamental aspects to consider when designing the support system in a rockburst prone areas. The study reported that depth of fracturing is one of the major aspects to be considered in order to design relevant and useful support systems. Their argument was raised due to the fact that the PPV chart previously used during designing support systems was found to present fundamental error or unrealistic results. This followed a comparison between the damage and seismic event where these unrealistic results were noted at the PPV values to be less than 2. Therefore, these charts can be used as an alternative way to overcome such common fundamental errors pointed out by the authors (Cai and Kaiser 2018). In the final analysis, the chart has been found to be relevant when predicting the initiations of an extension fracture and its depth, where the chart can be used in both estimations of rib pillar stability and to estimate the quality of the support system to be installed in a brittle rock pillar with time.

## 5 Conclusions

The developed charts totally agreed with the empirical analysis (borehole periscope and GPR) and the developed equations. The charts indicate that extension fractures are developed in several stages which include; firstly, micro-fracture, secondly; closed fractures and finally; open fracture. These observations or results have been reported by several previous studies such as Adams and Jager (1980), Clotte et al. (1972–1973), Kuijpers (2000), van Aswegen and Stander (2012), Sengani and Zvarivadza (2018a). This has led to the conclusion that extension fractures mature with time. The maturity of fractures is quicker in a brittle heterogeneous rock pillar than in a homogenous rock pillar. This implies that the presence of seismic active geological features within a rock pillar has much more impact on the rate at which extension fractures can be initiated. As a result, there are several studies that

correspond with this conclusion such as Stacey (1981) who reported that the initiation of extension fractures depends on the characteristics of the rock type. Similarly, Borg and Maxwell (1956), Gallagher et al. (1974), the National Research Council (1996), also confirmed that the presence of geological features in a rock mass results into rock fracturing.

The study also noted that Stacey’s extension criterion (Stacey 1981) is obsolete related to the results of the study but there are some few fundamental adjustments which are needed to align the criterion. The criterion (Stacey’s extension criterion) seems to outline the behaviour of the homogenous brittle rock pillar with no visible seismic active fault rather than the heterogeneous brittle rock pillar with single or multiple seismic active faults. In other words, the criterion by Stacey (1981) generalises the initiation of extension fractures in a brittle rock mass regardless of the composition. Due to that limitation, it was then concluded that improved equations from Stacey (1981) should be proposed to accommodate the initiations of extension fractures at the different compositions of the brittle rock pillars. Therefore, the following modified Stacey’s extension criteria are presented in which it is believed that extension fractures are initiated when  $(\nu(\sigma_1 + \sigma_2) > \sigma_3) \times f_n$ , for a homogenous brittle rib pillar, also initiated  $(\nu(\sigma_1 + \sigma_2) > \sigma_3) \times f_s$ , for a heterogeneous brittle rib pillar with single seismic active fault and lastly  $(\nu(\sigma_1 + \sigma_2) > \sigma_3) \times f_m$ , for a heterogeneous brittle rib pillar. These equations are very simple to use, however the values of factors  $f_n$ ,  $f_s$  and  $f_m$  are constant values which are given as; 1 for  $f_n$ , 0.85 for  $f_s$  and 0.65 for  $f_m$ . These equations together with other analysis in the study made it possible to develop three time-dependent charts on the initiations of extension fractures in brittle rock pillars of different compositions in a high stress environment.

The charts were also proven to provide relevant practical application in most of the previous studies. The charts were noted to predict the stability of the rib pillar as time progressed and predicted the duration required to install support systems in an effective manner. In conclusion, although these charts are very relevant to the case studies outlined in the study, it is not expected that this chart becomes applicable in any brittle rock type or any stress levels. The charts are very useful in a brittle rock pillar at a high stress level in hard rock mining. The usefulness of understanding

the depth of fracturing and fracture initiations has been reported to be the most significant aspect when designing support systems in rockburst prone areas (Cai and Kaiser 2018) and also in a coal mine (long hole stoping) (Louchnikov 2011). Therefore, the charts are very useful in many applications. It is also suggested that further research on sophisticated methods related to these charts be developed.

**Acknowledgements** The author wishes all mineworkers who lost their lives as a result of rock burst accidents to rest in eternal peace.

#### Compliance with ethical standards

**Conflict of interest** The author wishes to confirm that there are no known conflicts of interest associated with this publication, there has been no financial support given to influence the outcome of this work.

#### References

- Adams GR, Jager AJ (1980) Petrosopic observations of rock fracturing ahead of stope faces in deep-level gold mines. *J S Afr Inst Min Metall* 80:204–209
- Andersson JC, Martin CD, Stille H (2009) The Aspö pillar stability experiment: part II—rock mass response to coupled excavation induced and thermal-induced stresses. *Int J Rock Mech Min Sci* 46:879–895
- Andrews P, Sengani F (2017) Ameliorating the strainburst risk in a mechanised deep level gold mine: the South Deep experience. In: *Strainburst in mining seminar 10th October 2017 Sudbury Canada*
- Andriev GE (1995) Brittle failure of rock materials. A. A. Balkema, Rotterdam
- Ashby MF, Hallam D (1986) The failure of brittle solids containing small cracks under compressive stress. *Acta Metall* 34:497–510
- Barton CC (1983) Systematic jointing in the Cardium Sandstone along the Bow River, Alberta, Canada. Ph.D. Thesis, Yale University, pp 200–301
- Bates RL, Jackson JA (1980) Glossary of geology, 2nd edn. American Geological Institute, Falls Church
- Borg IY, Maxwell JC (1956) Interpretation of fabrics of experimentally deformed sands. *Am J Sci* 254:71–81
- Brace WF (1960) An extension of the Griffith theory of fracture to rocks. *J Geophys Res* 65:3477–3480
- Brace WF (1964) Brittle fracture of rocks. In: Judd WR (ed) *State of stress in the earth's crust*. American Elsevier, New York, pp 111–180
- Brace WF, Byerlee JD (1968) Recent experimental studies of brittle fracture of rocks. In: Fairhurst CL (eds) *Proceedings of the 8th symposium on rock mechanics. Failure and Breakage of Rock*, pp 58–81
- Brace WF, Paulding B, Scholz C (1966) Dilatancy in the fracture of crystalline rocks. *J Geophys Res* 71:3939–3953
- Brady BHG, Brown ET (2004) *Rock mechanics for underground mining*, 3rd edn. Kluwer, Dordrecht, p 628
- Cai M, Kaiser PK (2018) Rockburst support. In: *Rockburst phenomenon and support characteristics*. MIRARCO—Mining Innovation, Laurentian University, Sudbury, Ontario, Canada
- Cai M, Kaiser PK, Martin CD (1998) A tensile model for the interpretation of microseismic events near underground openings. *Pure appl Geophys* 153:67–92
- Cho N, Martin CD, Sego DS (2007) A clumped particle model for rock. *Int J Rock Mech Min Sci* 44:997–1010
- Clausing DP (1959) Comparison of Griffith's theory with Mohr's failure criteria. *Colo Sch Mines* 54:255–296
- Clotte DR, Clotte PAG, Cooke NGW, Jager AJ, White AJA (1972–1973) The nature of the fractures zone in gold mines as revealed by diamond core drilling. In: *Association of mine managers, papers, and discussions*. Johannesburg
- De Kock WP (1964) The geology and economic significance of West Wits line. In: Houghton SH (ed) *Geology of some ore deposits in Southern Africa*. Geological Society of South Africa, Johannesburg
- Department of Mineral Resources (DMR) (2018) Annual incidents report. Pretoria, South Africa
- Dyer JR (1983) Jointing in sandstones, Arches National Park, Utah. Ph.D. Dissertation, Stanford University, Stanford, p 202
- Earon R, Olofsson B (2018) Hydraulic heterogeneity and its impact on kinematic porosity in Swedish coastal terrains. *Eng Geol* 245:61–71
- Erdogan F, Sih GC (1963) On the crack extension in plates under plane loading and transverse shear. *J Basic Eng* 85:519–525
- Fairhurst C (1964) On the validity of the “Brazilian” test for brittle materials. *Int J Rock Mech Min Sci Geomech Abstr* 1(4):535–546
- Fairhurst C (1972 and Updated in 2004) Fundamental considerations relating to the strength of rock. In: *Colloquium on rock fracture*. Bochum, Germany: Ruhr Universitat, <http://www.itascacg.com>
- Gallagher JJ, Friedman M, Handin J, Sowers GM (1974) Experimental studies relating to microfracture in sandstone. *Tectonophysics* 21:203–247
- Germanovich JN, Dyskin AV (1988) A model of brittle failure for material with cracks in uniaxial loading. *Mech Solids* 23:111–123
- Griffith AA (1921) The phenomena of rupture and flow in solids. *Philos Trans R Soc Lond (Ser A)* 221:163–198
- Griffith AA (1924) Theory of rupture. In: *Proceedings of the 1st international congress of applied mechanics*. Tech. Boekhandel en Drukkerij J Walter Jr, Delft, pp 55–63
- Hallbauer DK, Wagner H, Cook NGW (1973) Some observations concerning the microscopic and mechanical behaviour of quartzite specimens in stiff, triaxial compression tests. *Int J Rock Mech Min Sci Geomech Abstr* 10:713–726
- Hamm SY, Kim M, Cheong JY, Kim JY, Son M, Kim TW (2007) Relationship between hydraulic conductivity and fracture properties estimated from packer tests and borehole data in a fractured granite. *Eng Geol* 92:73–87
- Handin J, Heard HC, Magouirk JN (1967) Effects of the intermediate principal stress on the failure of limestone,

- dolomite and glass at different temperatures and strain rates. *J Geophys Res* 72:611–640
- Hedley DGF, Grant F (1972) Stope and pillar design at the Elliot Lake uranium mines. *CIM Bull* 65(723):37–44
- Hoek E (1964) Rock fracture around mine excavations. In: CSIR rock mechanics special report no. 38. International Conference on Strata Control and Rock Mechanics, New York
- Hoek E (1965) Rock fracture under static stress conditions. In: Council for Scientific and Industrial Research Report MEG. Pretoria, South Africa, p 383
- Hoek E, Brown ET (1980) Underground excavations in rock. IMM, London, p 527
- Hoek E, Martin CD (2014) Fracture initiation and propagation in intact rock—a review. *J Rock Mech Geotech Eng* 6:287–300
- Huang N, Jiang Y, Liu R, Li B (2017) Estimation of permeability of 3-D discrete fracture networks: an alternative possibility based on trace map analysis. *Eng Geol* 226:12–19
- Hudyma M (1988) Development of empirical rib pillar failure criterion for open stopemining. MASC Thesis, Department of Mining and Mineral Processing, University of British Columbia, Vancouver
- Inglis CE (1913) Stresses in a plate due to the presence of cracks and sharp corners. Institution of Naval Architects, London, pp 219–230
- Jaeger JC, Cook NGW, Zimmerman RW (2007) Fundamentals of rock mechanics. Blackwell, Victoria
- Kemeny JM, Cook NGW (1987) Crack models for the failure of rock under compression. In: Desai CS, Krempl E, Kioussis PD, Kundu T (eds) Proceedings of the 2nd international conference constitutive laws for engineering materials, theory and applications, vol 1. Elsevier Science Publishing Co., London, pp 879–887
- King RG, Jager AJ, Roberts MKCR (1989) Rock mechanics aspects of stoping without back area support. COMRO Res. Rep, Johannesburg
- Krauland N (1970) The behaviour of a prototype and a model mine tunnel. In: South African tunnelling conference. The Technology and Potential of Tunnelling, Johannesburg
- Krauland N, Soder PE (1987) Determining pillar strength from pillar failure observations. *Eng Min J* 8:34–40
- Kuijpers J (2000) Fracturing around highly stressed excavations in brittle rock. *J South Afr Inst Min Metall* 100:325–331
- Kwásniewski M, Takahashi M (2010) Strain-based failure criteria for rocks: state of the art and recent advances. In: Rock mechanics in civil and environmental engineering—Proceedings of the European rock mechanics symposium. EUROCK, pp 45–56
- Lawn BR, Wilshaw TR (1975) Fracture of brittle solids. Cambridge University Press, Cambridge, p 204
- Lee CH, Deng BW, Chang JL (1995) A continuum approach for estimating permeability in naturally fractured rocks. *Eng Geol* 39:71–85. [https://doi.org/10.1016/0013-7952\(94\)00064-9](https://doi.org/10.1016/0013-7952(94)00064-9)
- Li D, Wong LNY (2013) The Brazilian disc test for rock mechanics applications. *Rock Mech Rock Eng* 46:269–287
- Lim SS, Martin CD (2010) Core diskling and its relationship with stress magnitude for Lac Du Bonnet granite. *Int J Rock Mech Min Sci* 47:254–264
- Louchnikov V (2011) Simple calibration of the extension strain criterion for its use in numerical modelling. In: Potvin Y (ed) Strategic vs tactical approaches in mining. Australian Centre for Geomechanics, Perth, pp 85–96
- Lunder P (1994) Hard rock pillar strength estimation: an applied empirical approach. MASC Thesis, University of British Columbia, Vancouver, British Columbia, Canada, p 166
- Lunder P, Pakalnis R (1997) Determination of the strength of hard rock mine pillars. *CIM Bull* 90(1013):51–55
- Martin CD, Chandler NA (1994) The progressive fracture of Lac du Bonnet granite. *Int J Rock Mech Min Sci Geomech Abstr* 31:643–659
- Martin CD, Read RS, Martino JB (1997) Observations of brittle failure around a circular test tunnel. *Int J Rock Mech Min Sci* 34:1065–1073
- McCarthy T (2006) The Witwatersrand Supergroup. In: The geology of South Africa. Geological Society of South Africa/Council for Geoscience, Johannesburg, pp 155–186
- McClintock FA, Walsh J (1962) Friction on Griffith cracks in rocks under pressure. In: Proceedings of the 4th US national congress on applied mechanics. Berkeley, pp 1015–1021
- Murrell SAF (1958) The strength of coal under triaxial compression. In: Mechanical properties of non-metallic Brittle Materials. Butterworth Scientific Publications, pp 123–145
- Murrell SAF (1963) Criterion for brittle fracture of rocks and concrete under triaxial stress and the effect of pore pressure on the criterion. Pergamon Press, Oxford
- Murrell SAF (1965) The effect of triaxial stress systems on the strength of rocks at atmospheric temperatures. *Geophys J* 10:231–281
- National Research Council (1996) Rock fractures and fluid flow: contemporary understanding and applications. The National Academies Press, Washington, DC
- Ndlovu X (2006) Three dimensional analyses of stress and strain distributions around bord and pillar geometries. M.Sc. Eng Dissertation, University of the Witwatersrand
- Ndlovu X, Stacey TR (2007) Observations and analyses of roof guttering in a coal mine. *J S Afr Inst Min Metall* 107:477–492
- Nelson RA (1985) Geologic analysis of naturally fractured reservoirs. Gulf Publishing, Houston, p 320
- Nicksiar M, Martin CD (2012) Evaluation of methods for determining crack initiation in compression tests on low-porosity rocks. *Rock Mech Rock Eng* 45:607–617
- Orowan E (1949) Fracture and strength of solids. *Rep Prog Phys Phys Soc* 12:182–232
- Pan JB, Lee CC, Lee CH, Yeh HF, Lin HI (2010) Application of fracture network model with crack permeability tensor on flow and transport in fractured rock. *Eng Geol* 116:166–177
- Pang SS, Goldsmith W (1990) Investigation of crack formation during loading of brittle rock. *Rock Mech Rock Eng* 23:53–63
- Paterson MS, Wong TF (2005) Experimental rock deformation—the brittle field, 2nd edn. Springer, New York
- Peng SS, Johnson AM (1972) Crack growth and faulting in cylindrical specimens of Chelmsford granite. *Int J Rock Mech Min Sci Geomech Abstr* 9:37–86
- Pollard DD, Aydin A (1988) Progress in understanding jointing over the past century. *Geol Soc Am Bull* 100:1181–1204

- Pretorius DA (1964) The geology of the Central Rand goldfields. In: Houghton SH (ed) The geology of some ore deposits in Southern Africa, vol 1. Geological Society of South Africa, Johannesburg, pp 63–108
- Pretorius DA (1986) The Witwatersrand Basin: surface and subsurface geology and structure (map). In: Anhaeusser CR, Maske S (eds) Mineral deposits of Southern Africa, vol 1. Geological Society of South Africa, Johannesburg
- Reeves DM, Parashar R, Pohll G, Carroll R, Badger T, Wiloughby K (2013) The use of discrete fracture network simulations in the design of horizontal hillslope drainage networks in fractured rock. *Eng Geol* 163:132–143
- Ren XW, Santamarina JC (2018) The hydraulic conductivity of sediments: a pore size perspective. *Eng Geol* 233:48–54
- Ren F, Ma G, Fu G, Zhang K (2015) Investigation of the permeability anisotropy of 2D fractured rock masses. *Eng Geol* 196:171–182
- Ren F, Ma G, Fan L, Wang Y, Zhu H (2017) Equivalent discrete fracture networks for modelling fluid flow in highly fractured rock mass. *Eng Geol* 229:21–30
- Rummel F (1971) Uniaxial compression tests on right angular rock specimens with central holes Rock Fracture. In: Proceedings of the international symposium on rock mechanics, vol 2. Nancy, pp 90–101
- Ryder JA, Jager AJ (2002) A textbook on rock mechanics for hard rock mines. In: SIMRAC, Safety in Mines Research Advisory Committee, South Africa
- Salamon MDG (1970) Stability, instability and the design of mine workings. *Int J Rock Mech Min Sci* 7:613–631
- Scholz CH (1968) Microfracturing and the inelastic deformation of rock in compression. *J Geophys Res* 73:1417–1432
- Segall P, Pollard DD (1983a) Joint formation in granitic rock of the Sierra Nevada. *Geol Soc Am Bull* 94:563–575
- Segall P, Pollard DD (1983b) Nucleation and growth of strike-slip faults in granite. *J Geophys Res* 88:555–568
- Sengani F (2018a) Trials of the Garford hybrid dynamic bolt reinforcement system at a deep level gold mine in South Africa. *J South Afr Inst Min Metall* 118:289–296
- Sengani F (2018b) The performance of bolt-reinforced and shotcreted in-stope pillar in rockburst-prone areas. *Int J Min Geo-Eng* 52:105–117
- Sengani F, Amponsah-Dacosta F (2018) The application of the face-perpendicular preconditioning technique for destressing seismically active geological structures. *Min Technol* 12:241–255
- Sengani F, Kataka MO (2017) A comparison of the effectiveness of the roof-bolter and standard drill rig for the installation of long anchors in hard-rock mines. In: Proceedings of 3rd young professional's conference, Innovation Hub, Pretoria, 9–10 March 2017. Southern African Institute of Mining and Metallurgy, Johannesburg
- Sengani F, Zvarivadza T (2017) Review of pre-conditioning practice in mechanized deep to ultra-deep level gold mining. In: 26th International symposium on mine planning and equipment selection. Lulea University, Sweden, pp 29–31
- Sengani F, Zvarivadza T (2018a) Borehole periscope observations of rock fracturing ahead of the preconditioned mining faces in a deep level gold mine. In: 1st International conference on advances in rock mechanics. International Society for Rock Mechanics and Rock Engineering, TuniRock
- Sengani F, Zvarivadza T (2018b) Yielding support systems in deep to ultra-deep level gold mining. In: 1st International conference on advances in rock mechanics. International Society for Rock Mechanics and Rock Engineering, TuniRock
- Sengani F, Zvarivadza T (2018c) The use of face perpendicular preconditioning technique to destress a dyke located 60 m ahead of mining faces. In: Geomechanics and geodynamics of rock masses, volume 1: proceedings of the 2018 European rock mechanics symposium. CRC Press, p 417
- Sjöberg J (1992) Failure modes and pillar behaviour in the Zinkgruvan mine. In: Tillerson JR, Wawersik WR (eds) Proceedings of the 33rd US Rock mechanics symposium, 3–5 June. A. A. Balkema, Santa Fe, New Mexico, Rotterdam, pp 491–500
- Stacey TR (1981) A simple extension strain criterion for fracture of brittle rock. In: International journal of rock mechanics and mining sciences, 18
- Stacey TR (1982) Contribution to the mechanism of core discing. *J S Afr Inst Min Metall* 82:269–274
- Stacey TR (1989) Boring in massive rocks—rock fracture problems. In: Proceedings of the seminar on mechanised underground excavation. South African National Council on Tunnelling, pp 87–90
- Stacey TR, Harte ND (1989) Deep level raise boring—prediction of rock problems. In: Maury V, Fourmaintraux D, Balkema AA (eds) Proceedings of the international symposium rock at great depth, vol 2. pp 583–588
- Stacey TR, Yathavan K (2003) Examples of fracturing at very low stress levels. In: Proc. 10th Int. Cong. Int. Soc. Rock Mech., Sandton, S. Afr. Nat. Inst. For Rock Engng and S. Afr. Inst. Min. Metall., vol 2, pp 1155–1159
- Stacey TR, Yu X, Armstrong R, Keyter GJ (2003) New slope stability considerations for deep open pit mines. *J S Afr Inst Min Metall* 103:373–389
- Stacey TR, Ortlepp WD, Ndlovu X (2007) Dynamic rock failures due to ‘high’ stress at shallow depth. In: Proceedings of the 4th international seminar on deep and high stress mining. Australian Centre for Geomechanics, Perth, pp 193–204
- Steffanizzi S, Barla G, Kaiser PK (2007) Numerical modelling of strain driven fractures around tunnels in layered rock masses. In: Ribeiro, Olalla, Grossmann (eds) 11th Congress of the International Society for Rock Mechanics. Taylor and Francis Group, London, pp 971–974
- Toper AZ (2003) The effect of blasting on the rockmass for designing the most effective preconditioning blasts in deep level gold mines [Ph.D. Thesis]. University of the Witwatersrand, Johannesburg
- van Aswegen G, Stander M (2012) Origins of some fractures around tabular stopes in deep South African mines. *J S Afr Inst Min Metall* 112:729–735
- Villaescusa E (2014) Geotechnical design for sublevel open stoping. CRC Press, Boca Raton
- Von Kimmelman MR, Hyde B, Madgwick R J (1984) The use of computer applications at BCL Limited in planning pillar extraction and the design of mining layouts. In: Brown ET, Hudson JA (eds) Proceedings of the ISRM international

- symposium on design and performance of underground excavations, Cambridge, 3–6 September, pp 53–63
- Waldeck HG (1979) The design and support of large underground chambers at depth in the mines of the Gold Fields Group of South Africa. In: Proceedings of the 4th Congress International Society for Rock Mechanics. Montreux, pp 565–571
- Watson BP, Pretorius W, Mpunzi P, du Plooy M, Matthysen K, Kuijpers JS (2014) Design and positive financial impact of crush pillars on mechanized deep-level mining at South Deep Gold Mine. *J S Afr Inst Min Metall* 114:863–865
- Wei L, Liu Q, Liu X (2018) An improved crack initiation stress criterion for brittle rocks under confining stress. In: IOP Conference series: earth and environmental science, pp 1–16
- Wesseloo J, Stacey TR (2016) A reconsideration of the extension strain criterion for fracture and failure of rock. *Rock Mech Rock Eng* 49:4667–4679
- Xu C, Fidelibus C, Dowd P, Wang Z, Tian Z (2018) An iterative procedure for the simulation of the steady-state fluid flow in rock fracture networks. *Eng Geol* 242:160–168
- Zhang C, Chen Q, Qin X, Hong B, Meng W, Zhang Q (2017) In-situ stress and fracture characterization of a candidate repository for spent nuclear fuel in Gansu, northwestern China. *Eng Geol* 231:218–229
- Zhao G, Johnson AM (1992) Sequence of deformations recorded in joints and faults, Arches National Park, Utah. *J Struct Geol* 14:225–236
- Zhou S, Zhuang X, Rabczuk T (2018) A phase-field modeling approach of fracture propagation in poroelastic media. *Eng Geol* 240:189–203
- Zvarivadza T, Sengani F (2018a) Calibration of yielding pillar performance in deep level gold mines. In: 1st International conference on advances in rock mechanics. International Society for Rock Mechanics and Rock Engineering, TuniRock
- Zvarivadza T, Sengani F (2018b) Evaluation of in-stope pillar failure: a case study of deep to ultra-deep level gold mining in South Africa. In: Proceedings of the 3rd international conference on rock dynamics and applications (RocDyn-3), June 26–27. CRC Press, Trondheim, pp 675–680
- Zvarivadza T, Sengani F, Adoko AC (2017) In-stope pillar scaling and fracturing in Southern African deep level gold mining. In: 26th International symposium on mine planning and equipment selection. Luleå University, Sweden, pp 379–388

**Publisher's Note** Springer Nature remains neutral with regard to jurisdictional claims in published maps and institutional affiliations.